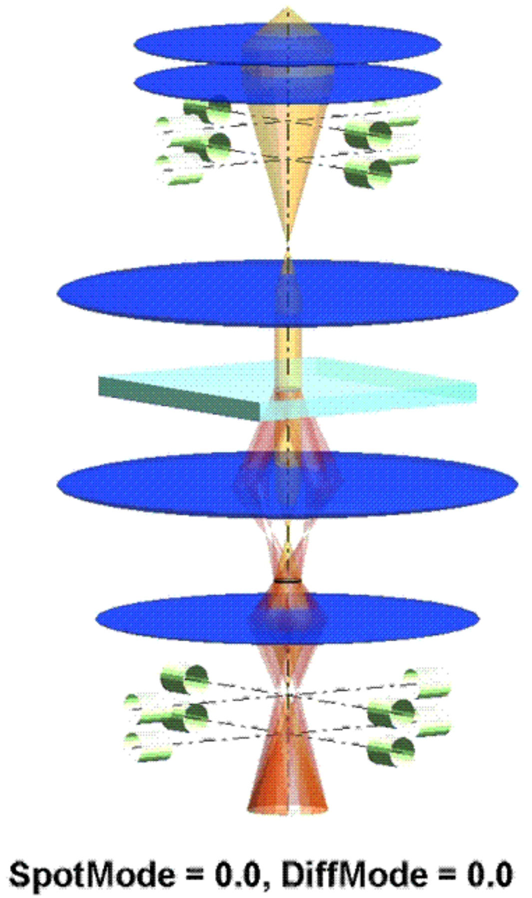

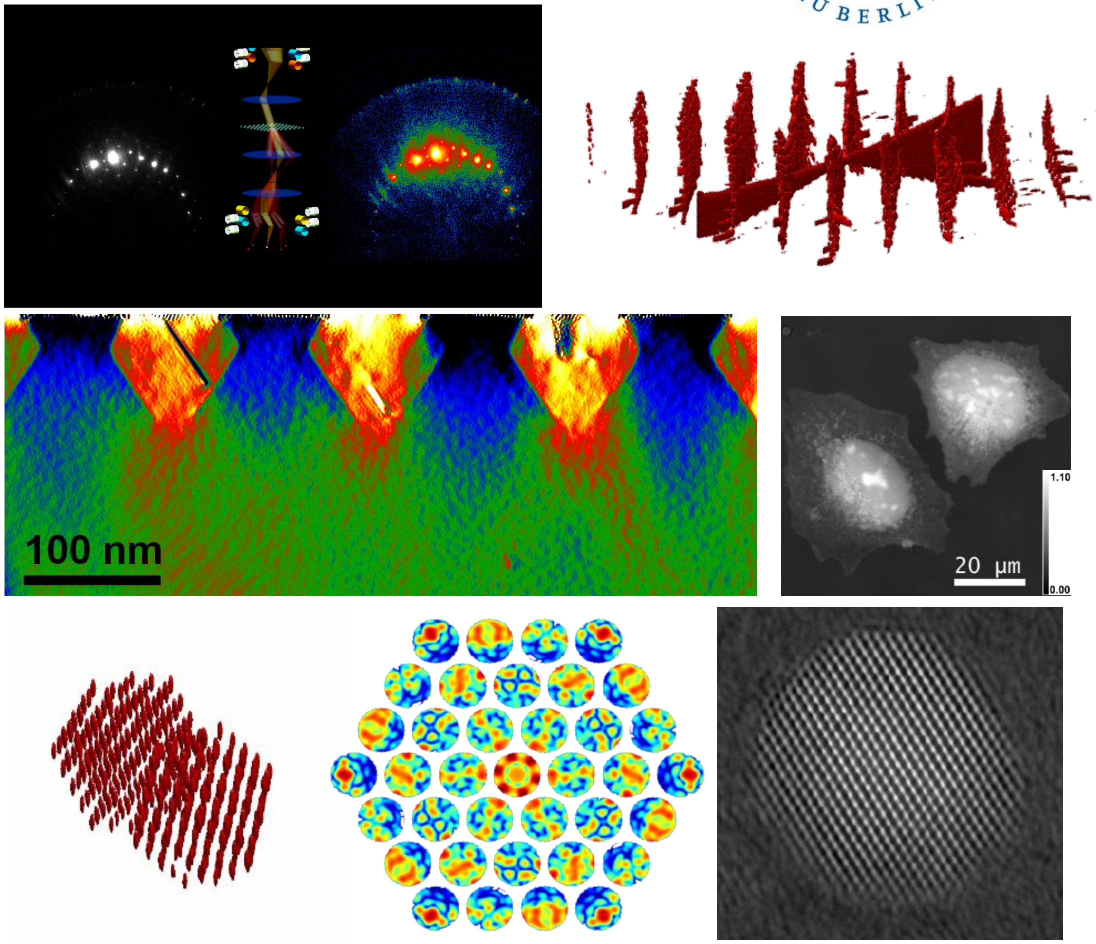

C.T. Koch | Humboldt University | Institut für Physik
Humboldt-Universität zu Berlin

Large angle methods and advanced techniques

Outline

1. Motivation
2. Precession Electron Diffraction (PED)
3. Aberration compensation
4. Large-Angle Rocking-Beam Electron Diffraction (LARBED)
5. Strain Mapping

Kinematical vs. Dynamical Scattering

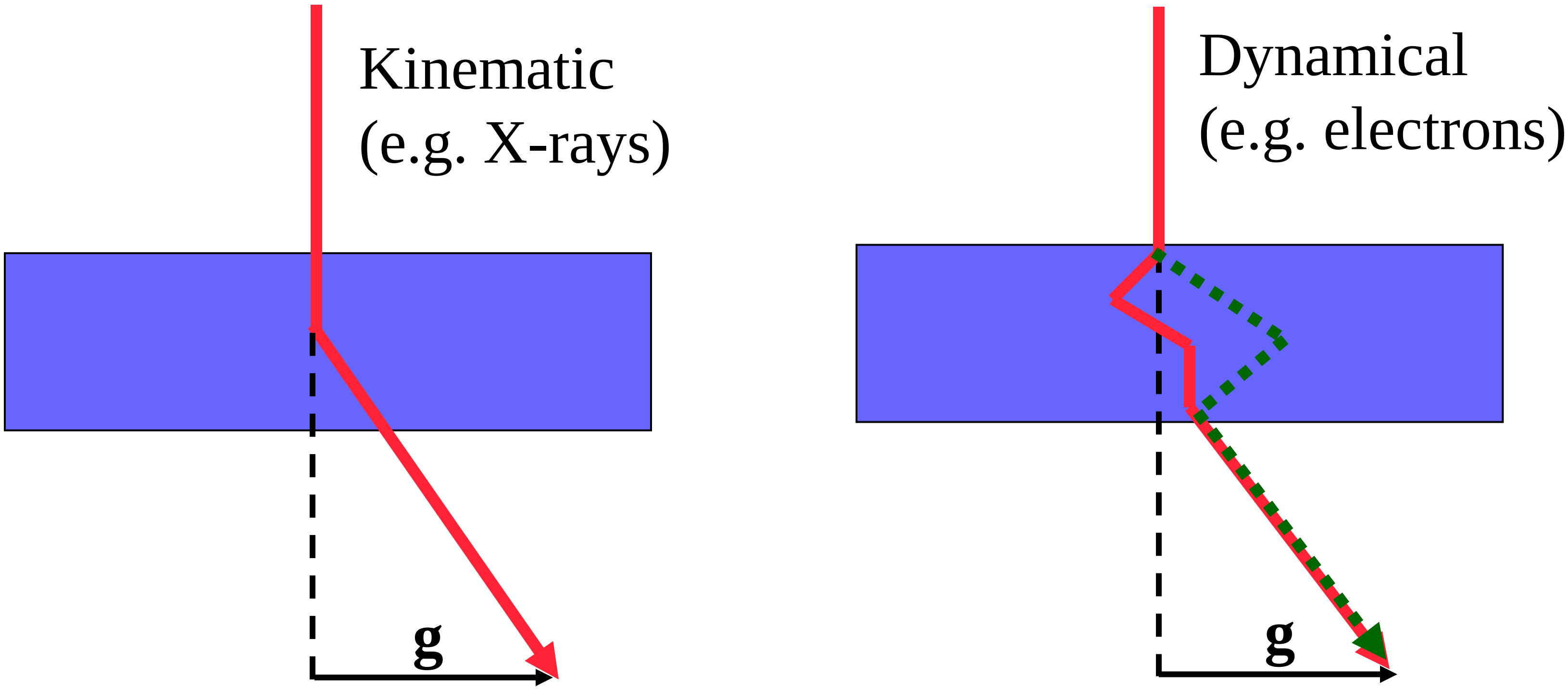

$$I(\vec{g}) \propto \left|F_g\right|^2 = \left|FT(\rho_z(\vec{r}))_g\right|^2 \qquad I(\vec{g}) \propto \left|\exp\left(i\pi\lambda t\,\underline{\underline{A}}[U(\vec{g})]\right)\right|_g^2$$

Kinematic Phase problem:

reconstruct $|F_g|$ -> ρ_z

$$U(\vec{g}) \propto FT(V(\vec{r}))$$

Electrons having traveled different paths within the crystal interfere!

Dynamical Scattering: Scattering Path Interference

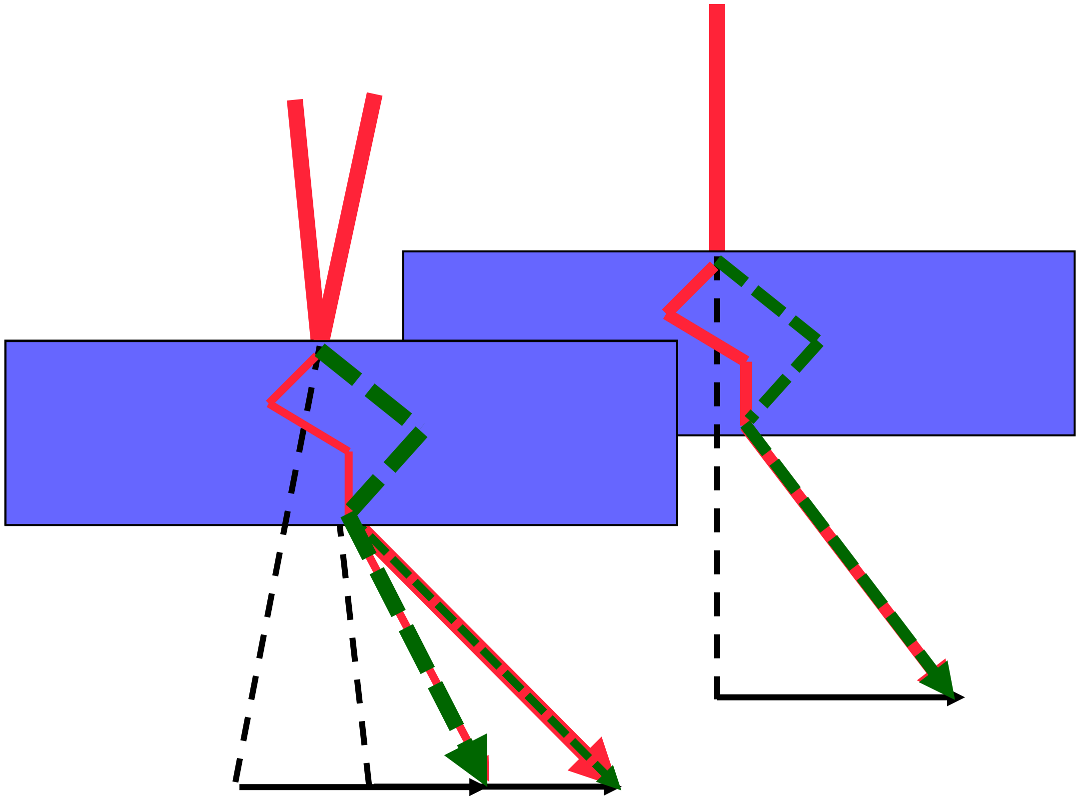

Convergent beam electron diffraction (CBED)

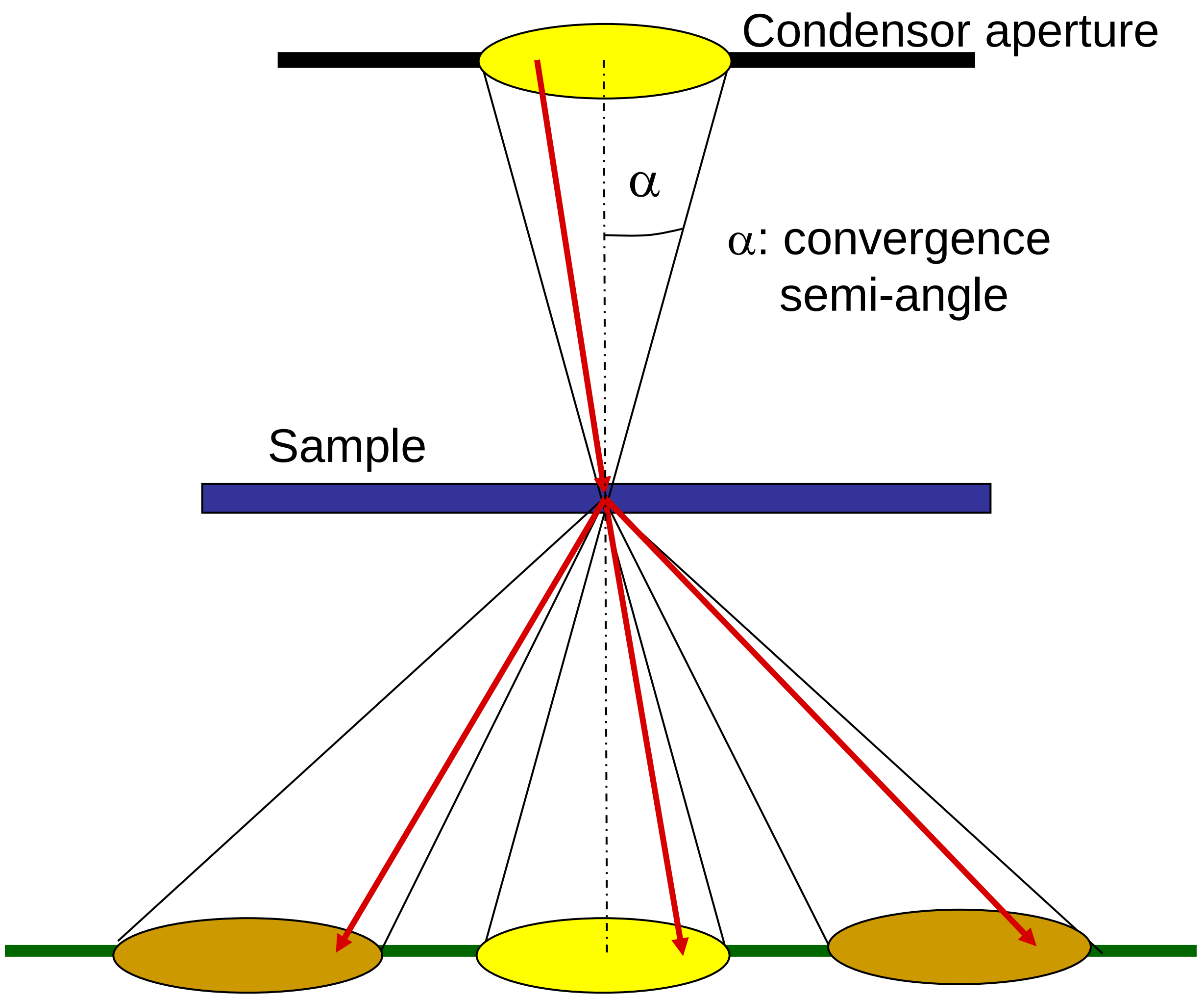

Each point in the diffraction pattern is a separate diffraction experiment, but they may all be recorded simultaneously.

CBED works well for small unit cell Xtals …

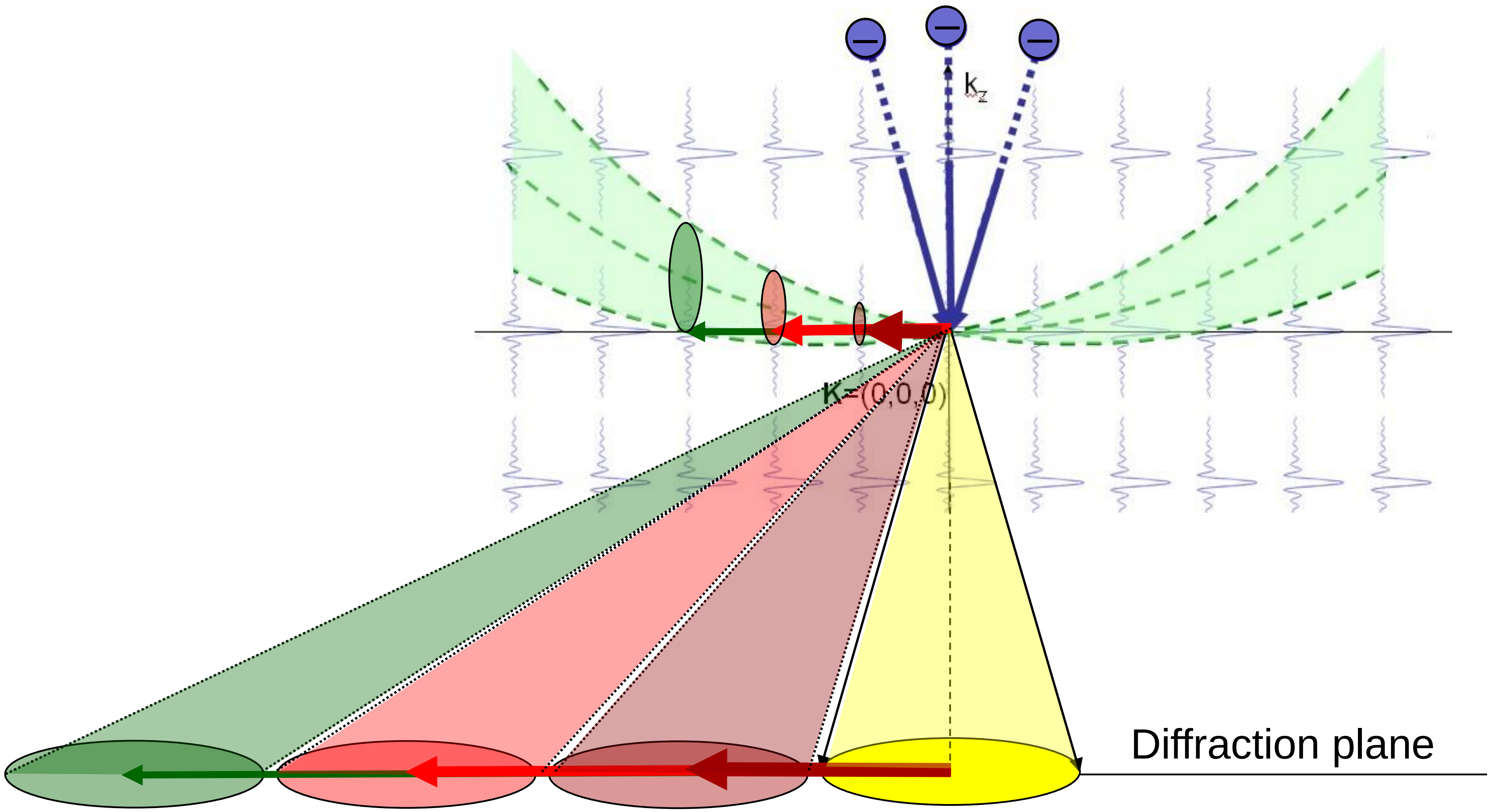

…but allows only tiny discs for large unit cells

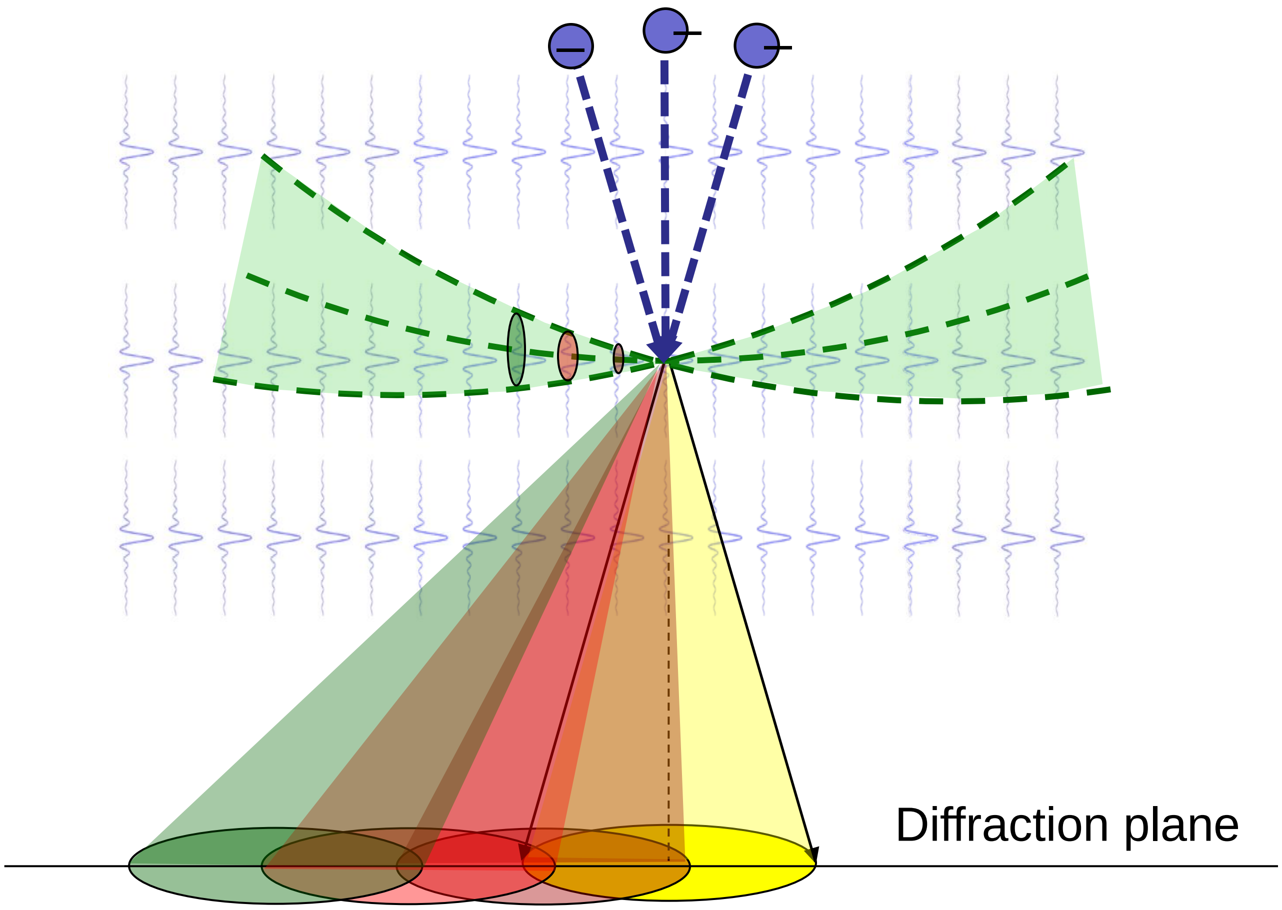

Also: Thin Samples Require Large Convergence Angles

CBED: Flat discs at low t => Need larger discs to get intensity variation

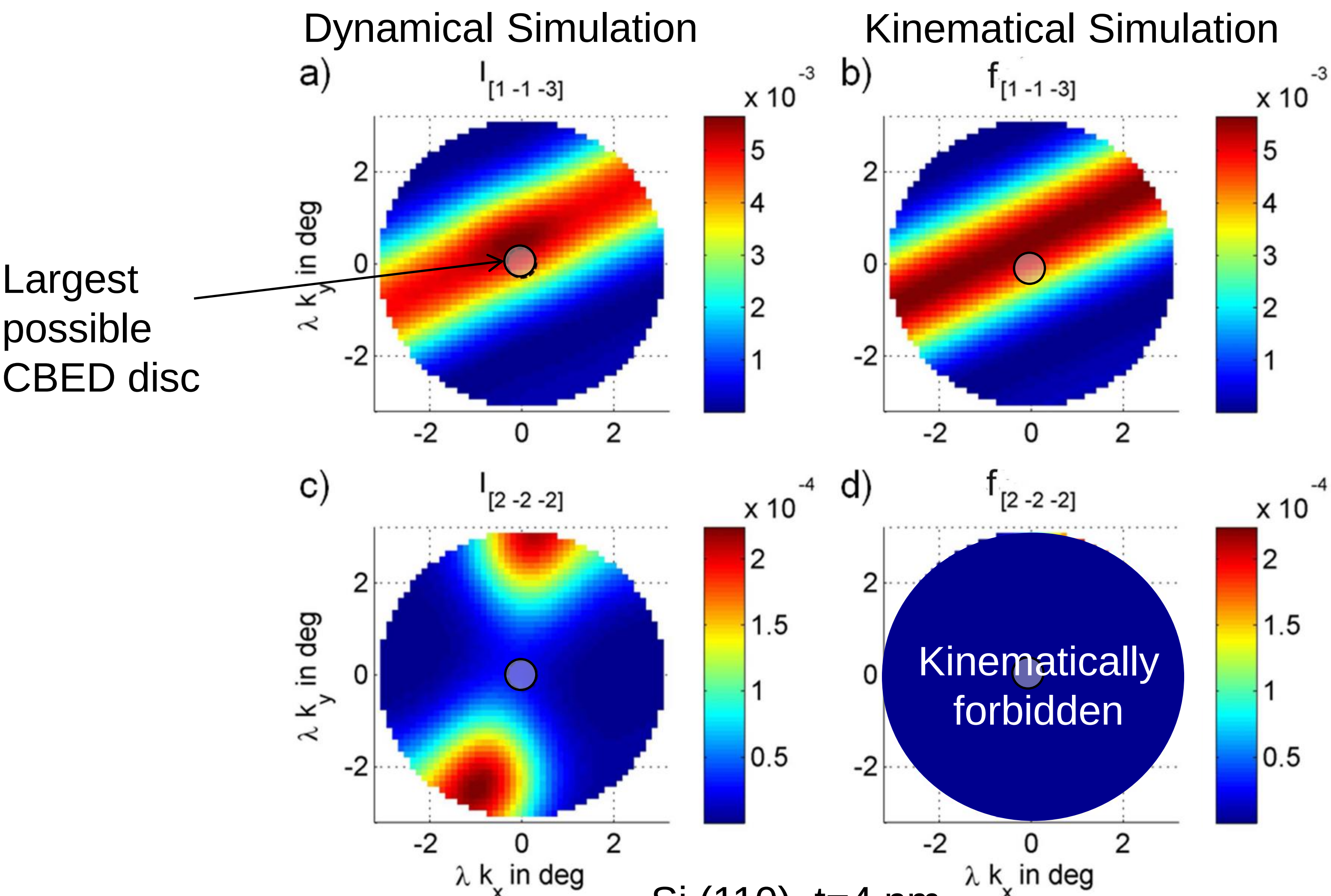

Si (110), t=4 nm

Dynamical Electron Diffraction is 4-Dimensional

‚Bragg line'

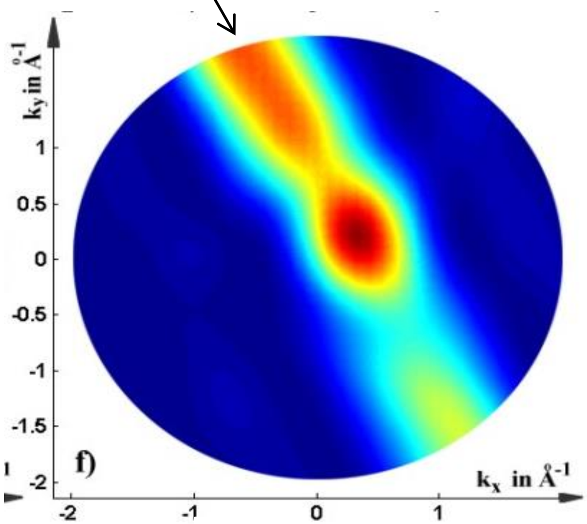

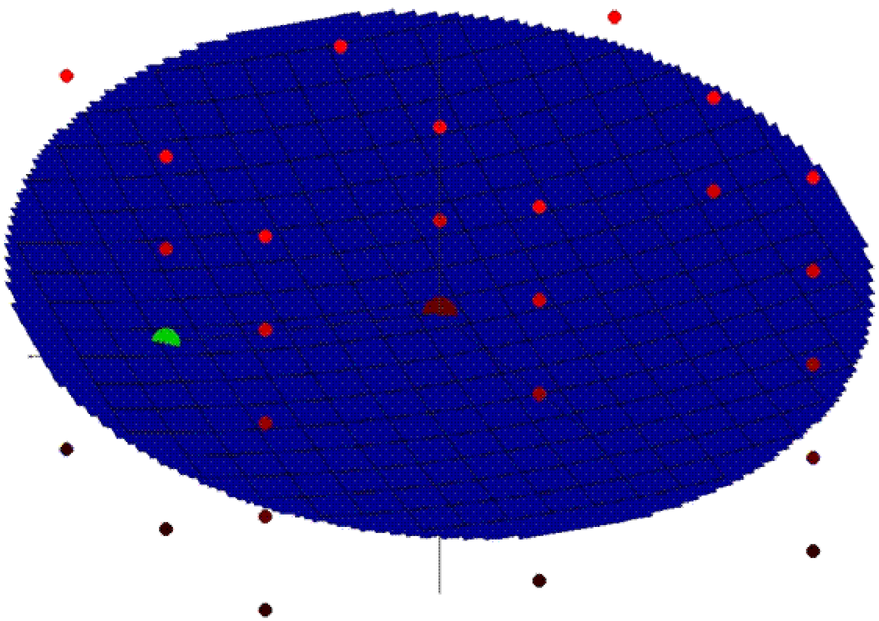

GaAs
g=[3$\bar{1}\bar{1}$]
E=200kV
t=70Å
17 beams

Any reflection can be in exact Bragg condition in a number of diffraction conditions
(as utilized in ‚reference beam X-ray diffraction' in a very rudimentary way)

Possible methods to increase the effective convergence angle

	CBED	DRZAP	LACBED	SLACBED	LACDIF	PED	Rotation	LARBED
Illuminated area	Small	Small	Large	Large	Large	Small	Small	Small
Tilt range	Small	Large	Large	Large	Large	Large	Large	Large
Shape of illumination	Disc	Square	Disc	Disc	Disc	Ring	Line	Disc/ring/any
Rocking info preserved	Yes	Yes	Yes	Yes	No	No	Yes	Yes
Whole diffraction pattern	Yes	No	No	Yes	Yes	Yes	Yes	Yes
Aberration compensation possible	No	Yes	No	No	No	Yes	Yes	Yes
Acquisition time	Short	Long	Long	Short	Short	Short	Long	(Long)

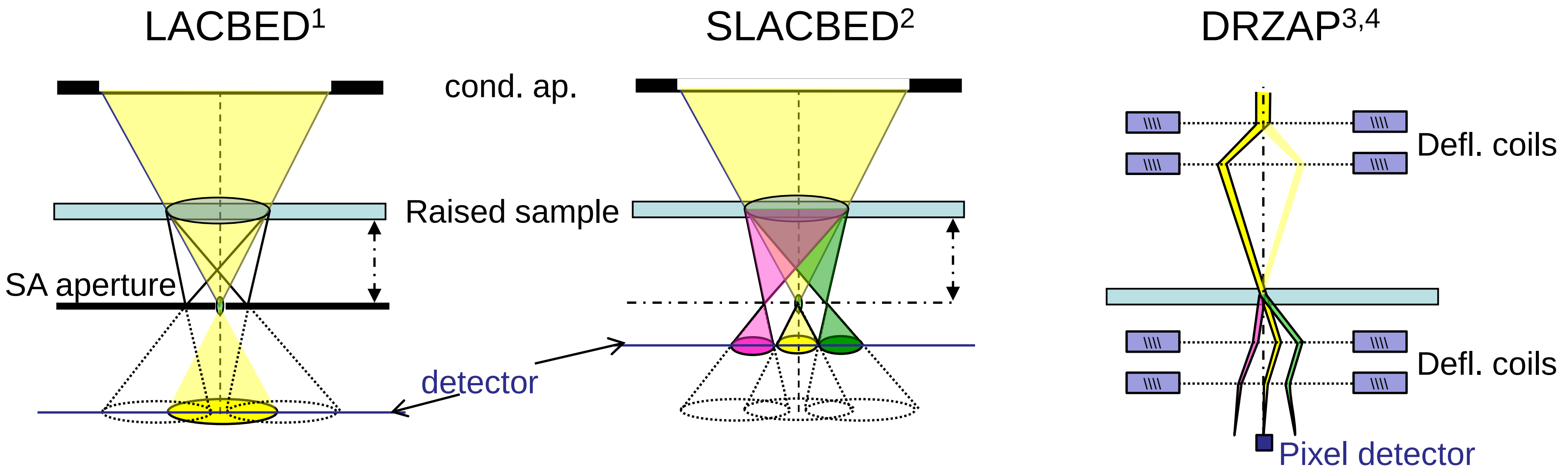

[1] M. Tanaka et al., J. Electron Microsc. 29 (4) (1980) 408
[2] M. Terauchi et al, J. Electron Microsc. 34 (1985) 128
[3] J.A. Eades, Ultramicr. 5 (1979) 71
[4] M. Tanaka et al., Jpn. J. Appl. Phys. 19 (1980) L201

Outline

1. Motivation
2. Precession Electron Diffraction (PED)
3. Aberration compensation
4. Large-Angle Rocking-Beam Electron Diffraction (LARBED)
5. Strain Mapping

Transmission Electron Diffraction

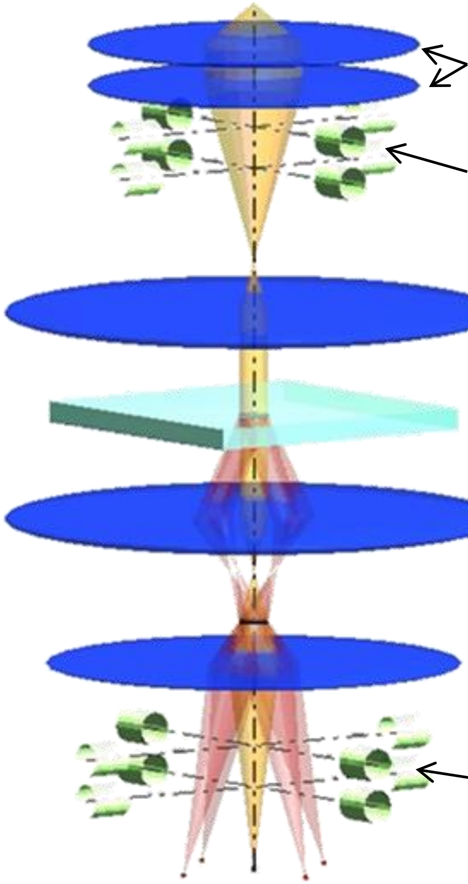

Rocking Beam Electron Diffraction

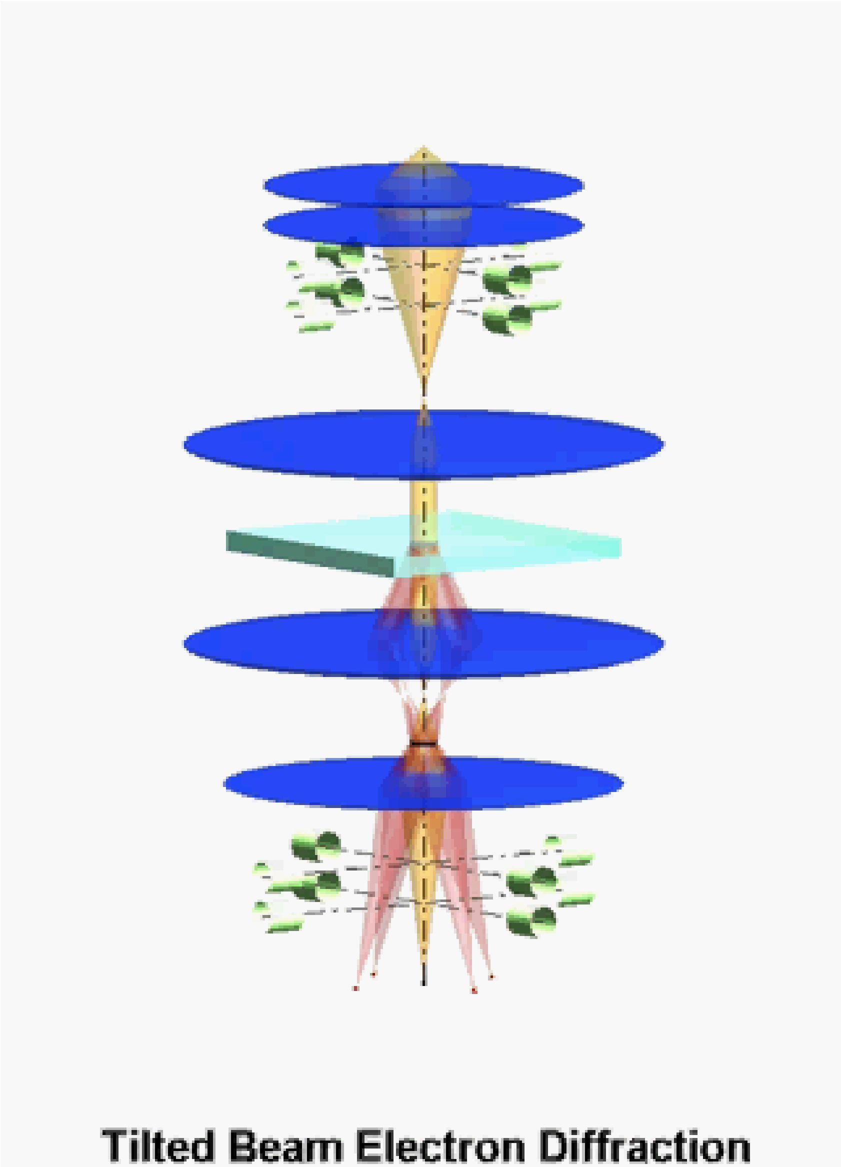

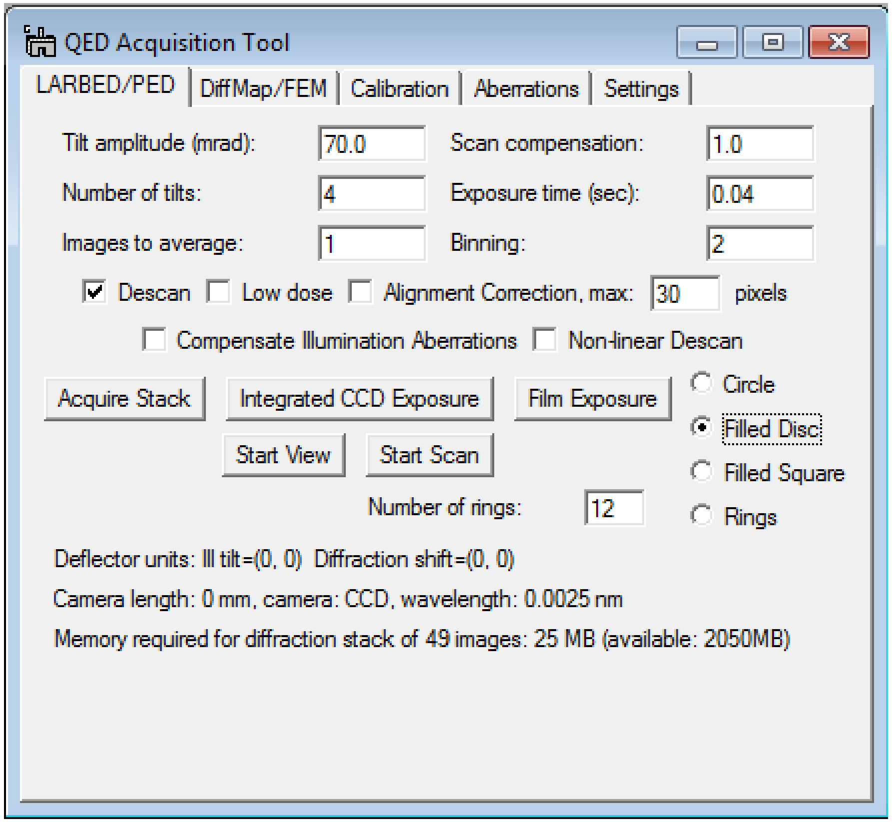

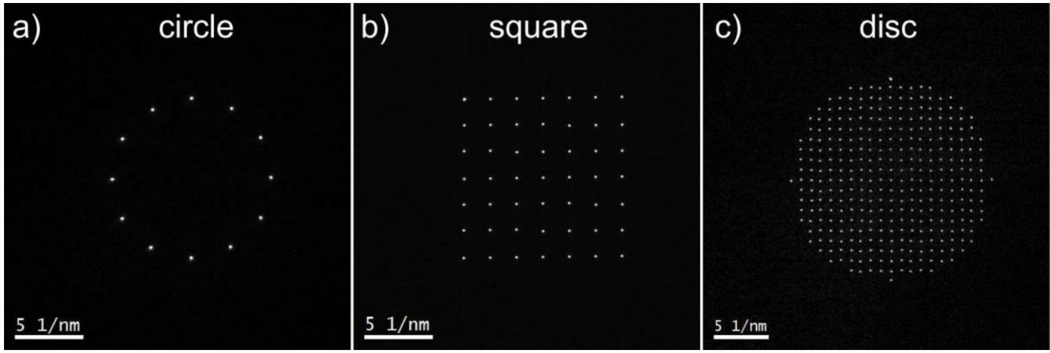

Precession Electron Diffraction (PED) of $SrTiO_3$ at 120 kV

Individual pattern

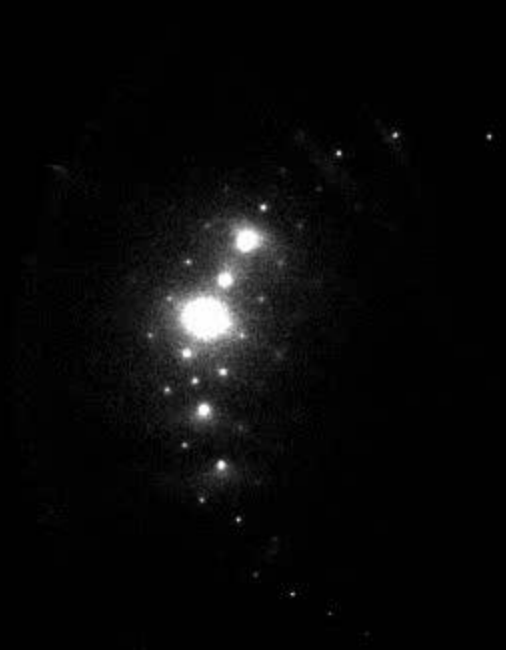

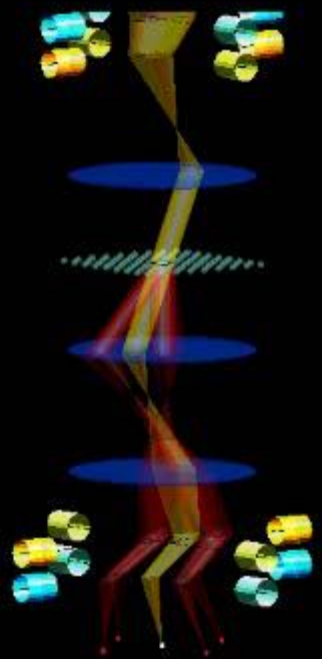

PED pattern

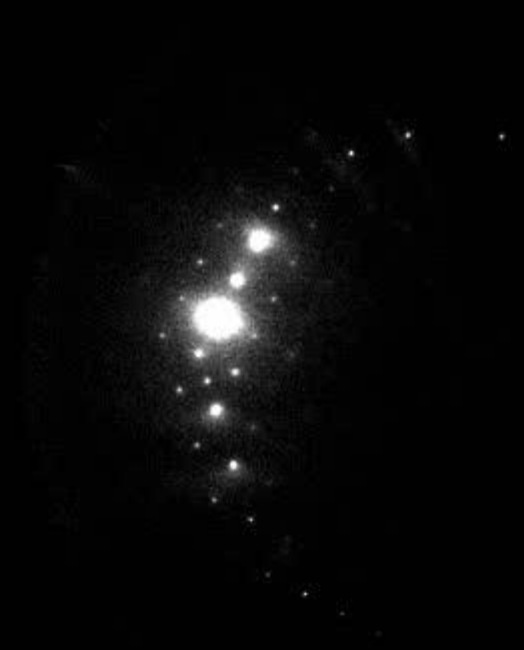

PED: R. Vincent, P. A. Midgley, Ultramicroscopy 53 (1994) 271

Automatically Acquiring Multiple Precession Angles θ

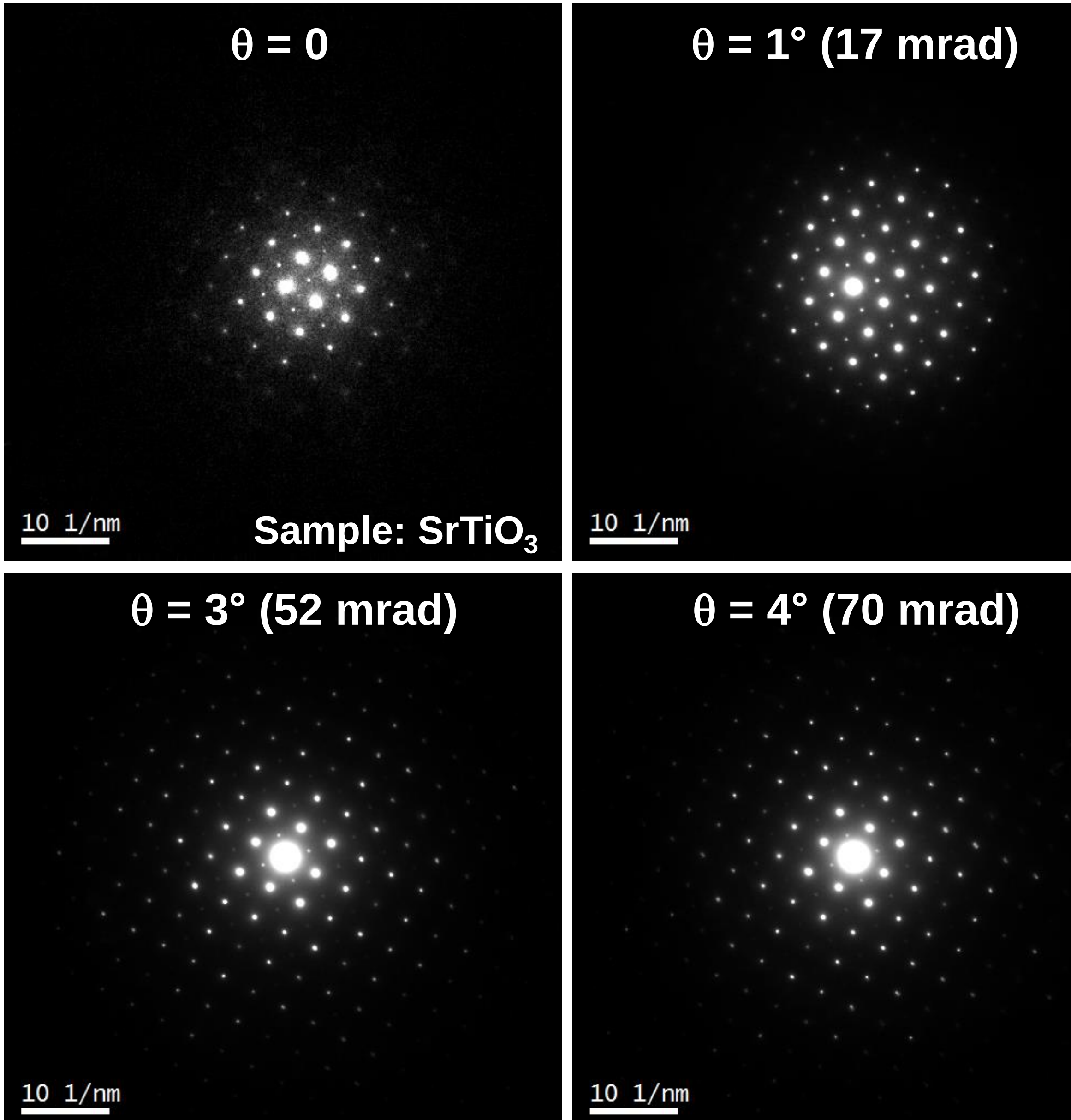

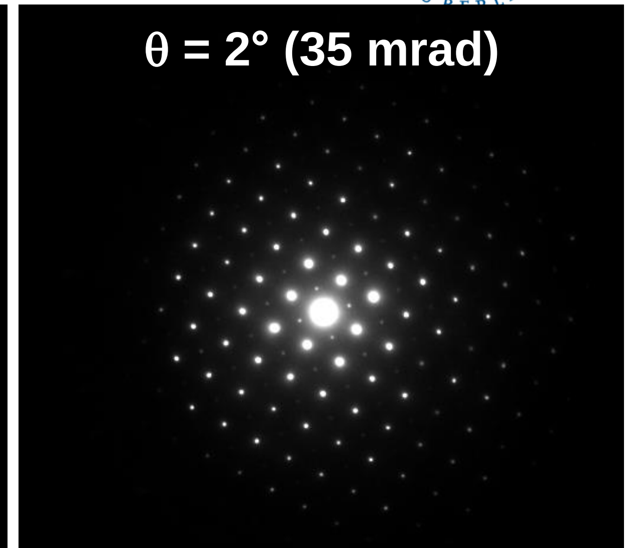

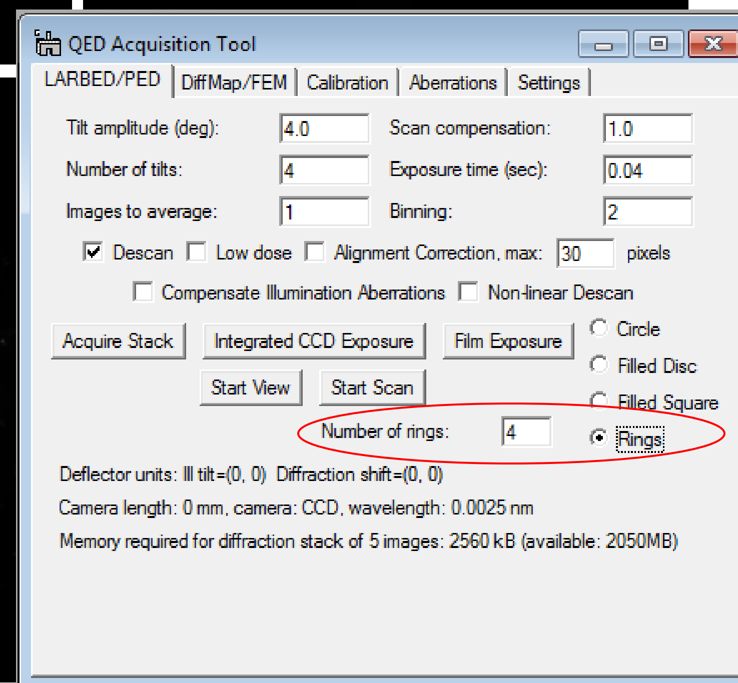

PED Pattern of $SrTiO_3$ (120 kV, 70 mrad, log scale)

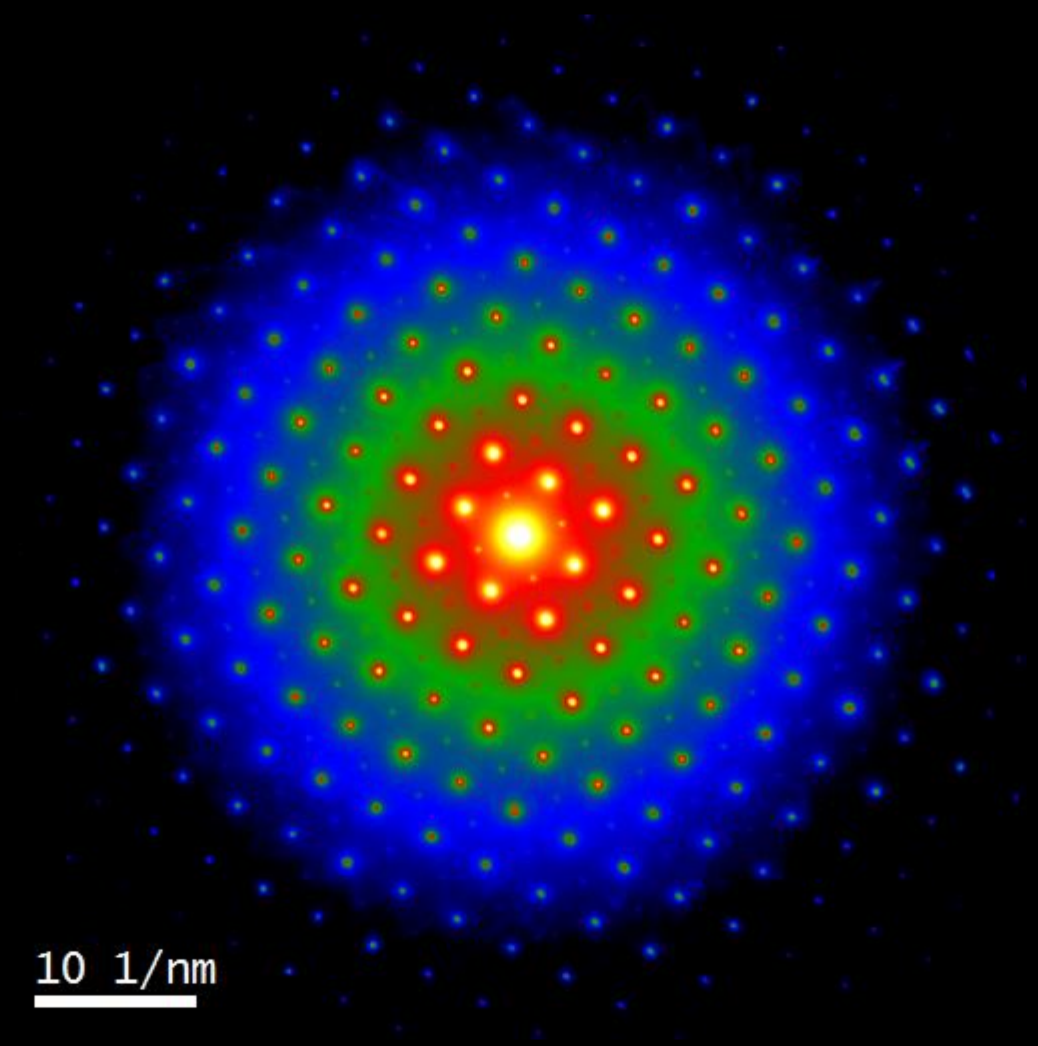

Automated Non-linear Calibration Refinement

Nonlinearities in the beam tilt or diffraction shift are automatically measured and taken into account during measurement.

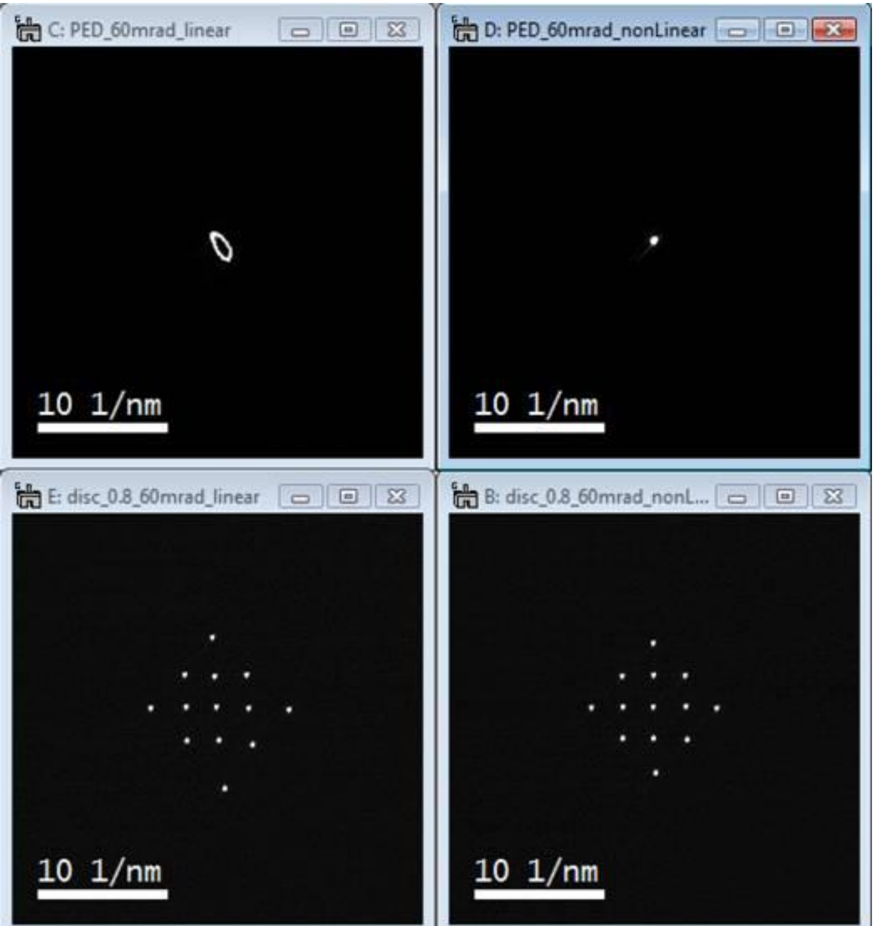

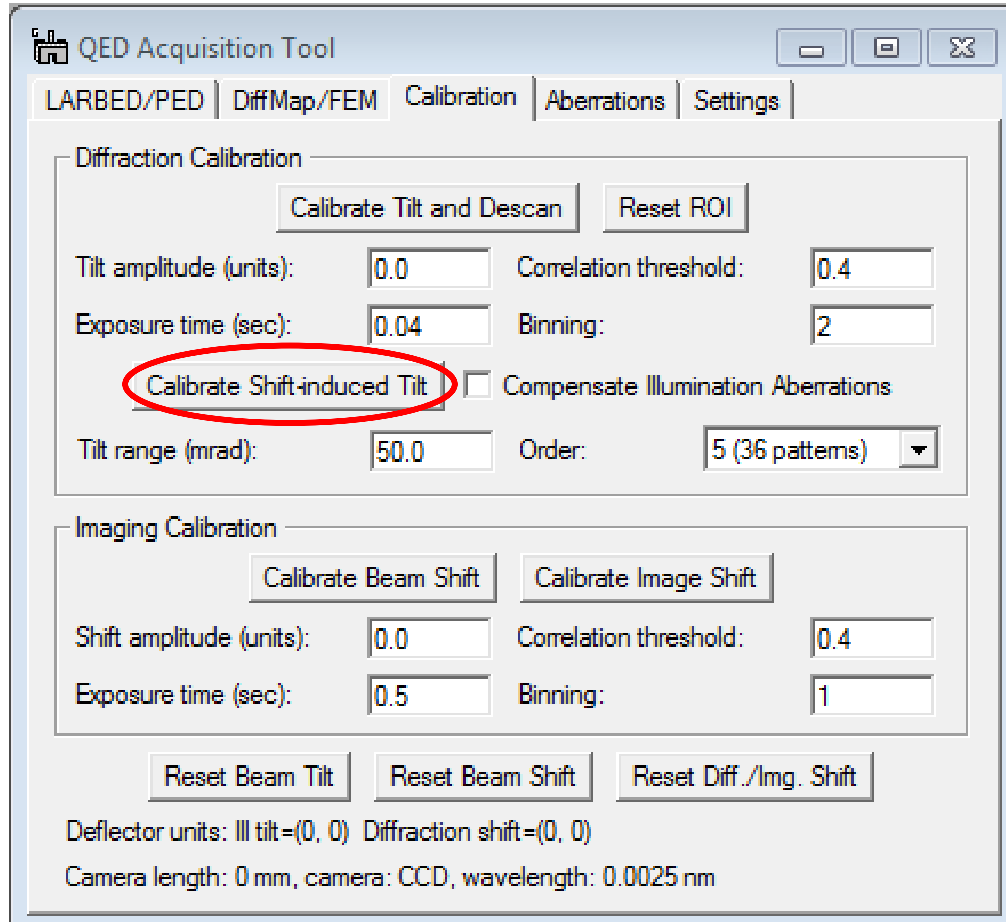

Even on systems facilitating this: Correcting scan distortions manually can take hours.

Outline

1. Motivation
2. Precession Electron Diffraction (PED)
3. Aberration compensation
4. Large-Angle Rocking-Beam Electron Diffraction (LARBED)
5. Strain Mapping

Aberrations of illumination system

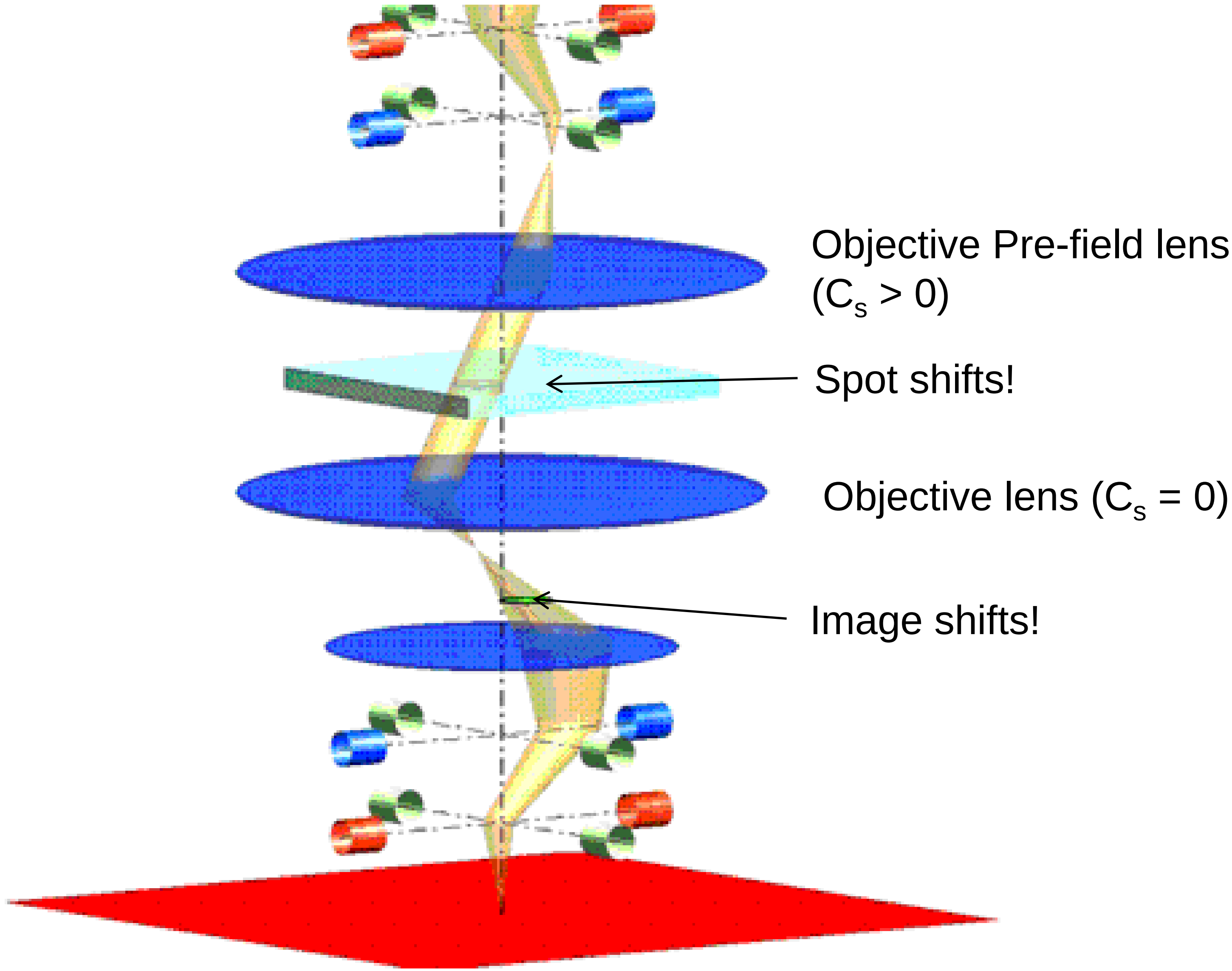

Measuring Aberrations in BF or DF mode

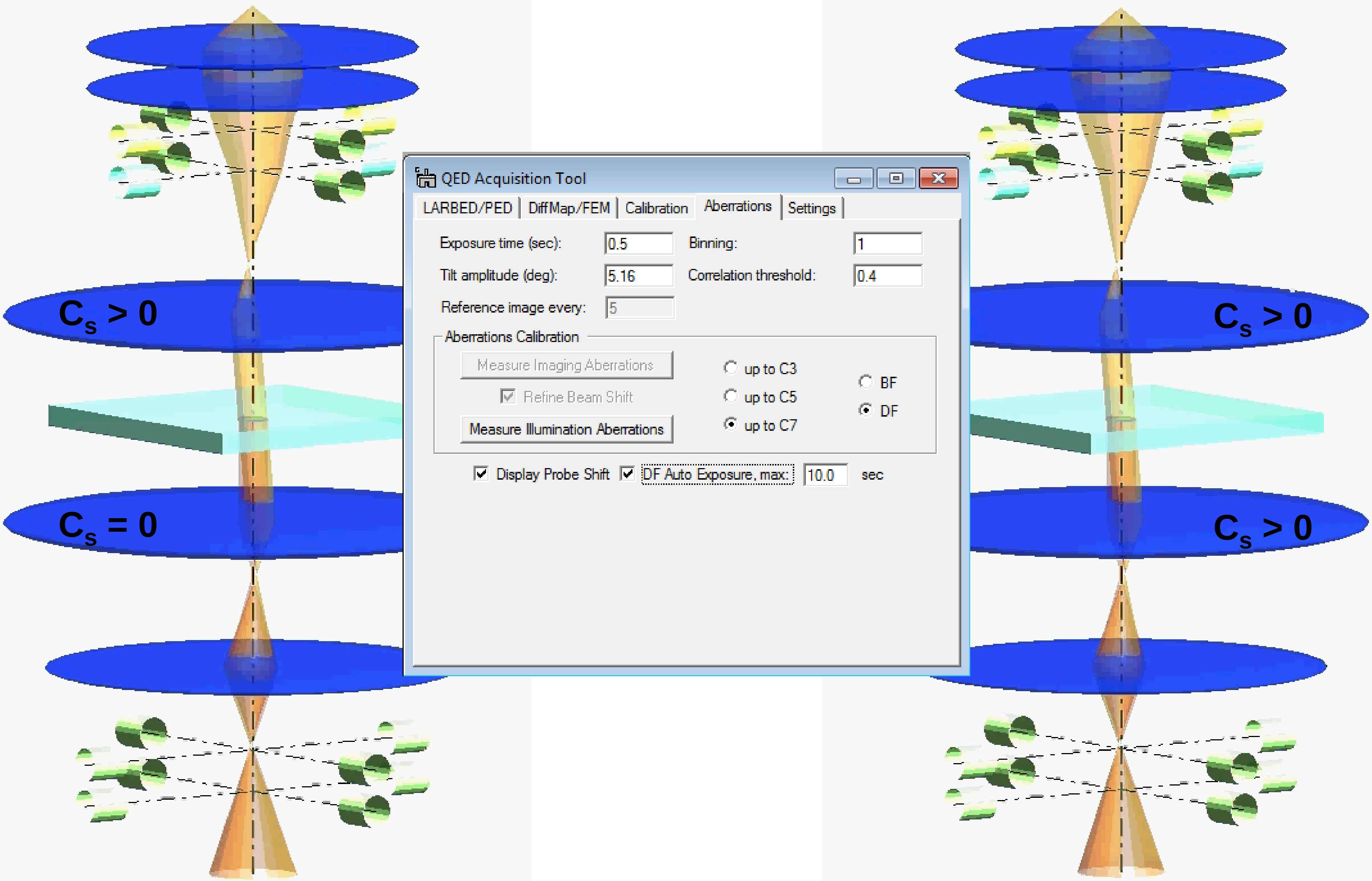

84 Pseudo Aberration Coefficients

Measuring illumination aberrations in BF mode requires first measuring img. aberrations.
Measuring illumination aberrations in DF mode may be more robust.

Coefficient	Obj. lens				OPF lens			
	a		b		a		b	
$C_{1,2}$ in nm	67.985	(25.5°)	352.531	(57.3°)	271.361	(44.5°)	2142.897	(−51.8°)
C_1 in nm	87.294	(−71.4°)			550.374	(−20.5°)		
$C_{2,3}$ in µm	10.285	(49.1°)	5.388	(122.7°)	8.678	(−171.0°)	11.585	(−24.7°)
$C_{2,1}$ in µm	85.280	(−33.7°)	75.057	(−165.7°)	69.669	(−73.9°)	208.362	(170.3°)
$C_{3,4}$ in mm	0.146	(−3.3°)	0.174	(−79.1°)	0.083	(51.4°)	0.367	(48.0°)
$C_{3,2}$ in mm	1.156	(161.5°)	0.254	(123.0°)	0.390	(−113.6°)	0.282	(13.7°)
C_3 in mm	11.313	(−8.8°)			12.893	(−12.5°)		
$C_{4,5}$ in mm	1.011	(109.6°)	0.972	(10.8°)	0.772	(−179.4°)	1.605	(−172.6°)
$C_{4,3}$ in mm	8.194	(175.7°)	11.211	(−5.8°)	8.813	(−5.4°)	15.019	(168.2°)
$C_{4,1}$ in mm	11.714	(143.5°)	5.086	(38.4°)	13.333	(−20.0°)	6.001	(−90.0°)
$C_{5,6}$ in mm	10.778	(−84.5°)	8.310	(151.7°)	16.919	(122.5°)	19.914	(18.2°)
$C_{5,4}$ in mm	113.401	(163.2°)	113.655	(69.4°)	54.582	(−93.8°)	286.811	(−144.0°)
$C_{5,2}$ in mm	348.752	(−30.2°)	113.381	(−34.7°)	179.911	(80.5°)	204.192	(176.7°)
C_5 in mm	191.765	(−58.4°)			241.600	(141.7°)		
$C_{6,7}$ in m	0.030	(59.4°)	0.021	(29.6°)	0.056	(−146.7°)	0.054	(−158.0°)
$C_{6,5}$ in m	0.244	(−82.9°)	0.254	(−169.2°)	0.324	(9.1°)	0.424	(9.2°)
$C_{6,3}$ in m	1.122	(−7.6°)	1.904	(174.9°)	1.435	(174.7°)	2.683	(−7.2°)
$C_{6,1}$ in m	1.234	(−30.4°)	0.414	(−166.5°)	1.596	(165.3°)	0.491	(100.2°)
$C_{7,8}$ in m	0.356	(19.2°)	0.413	(−36.9°)	0.369	(−149.1°)	0.244	(88.1°)
$C_{7,6}$ in m	1.464	(115.2°)	0.712	(−13.4°)	3.248	(−42.1°)	4.052	(−159.0°)
$C_{7,4}$ in m	14.676	(−23.0°)	15.428	(−127.3°)	7.786	(84.6°)	40.486	(28.1°)
$C_{7,2}$ in m	31.796	(141.3°)	17.140	(155.7°)	23.376	(−113.7°)	27.083	(−4.7°)
C_7 in m	12.367	(122.0°)			17.819	(−35.5°)		

QED automatically measures and compensates all these aberrations automatically

C. T. Koch, Ultramicroscopy **111** (2011) 832

Effect of Aberration Compensation

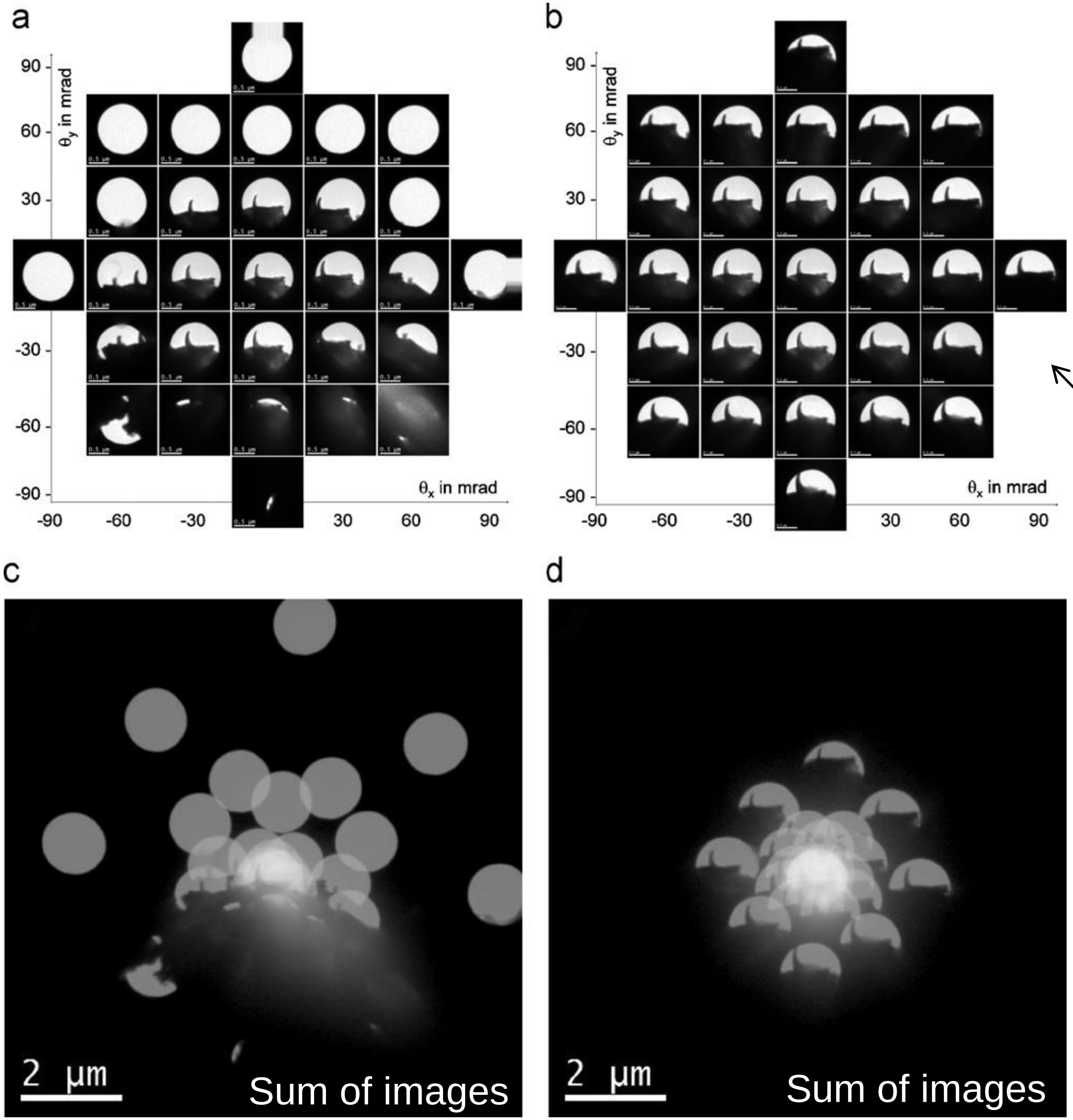

The Image moves on camera (imaging aberrations), but the spot is stationary on the sample

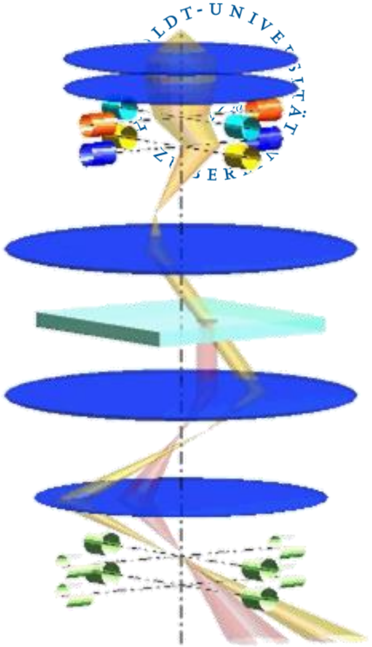

TEM: Zeiss EM912
θ_{max} = 90 mrad = 5.2°

Outline

1. Motivation
2. Precession Electron Diffraction (PED)
3. Aberration compensation
4. Large-Angle Rocking-Beam Electron Diffraction (LARBED)
5. Strain Mapping

Large-Angle Rocking-Beam Electron Diffraction

Individual pattern

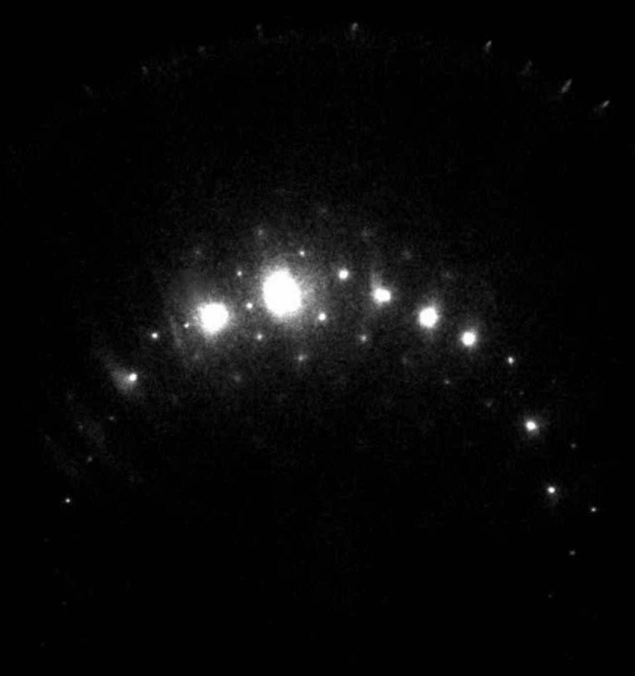

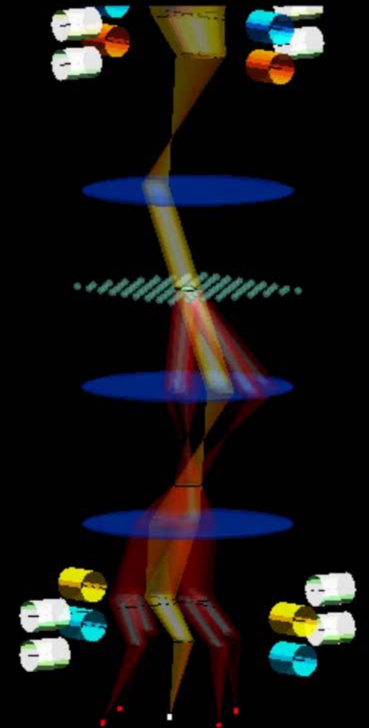

LARBED pattern (log scale)

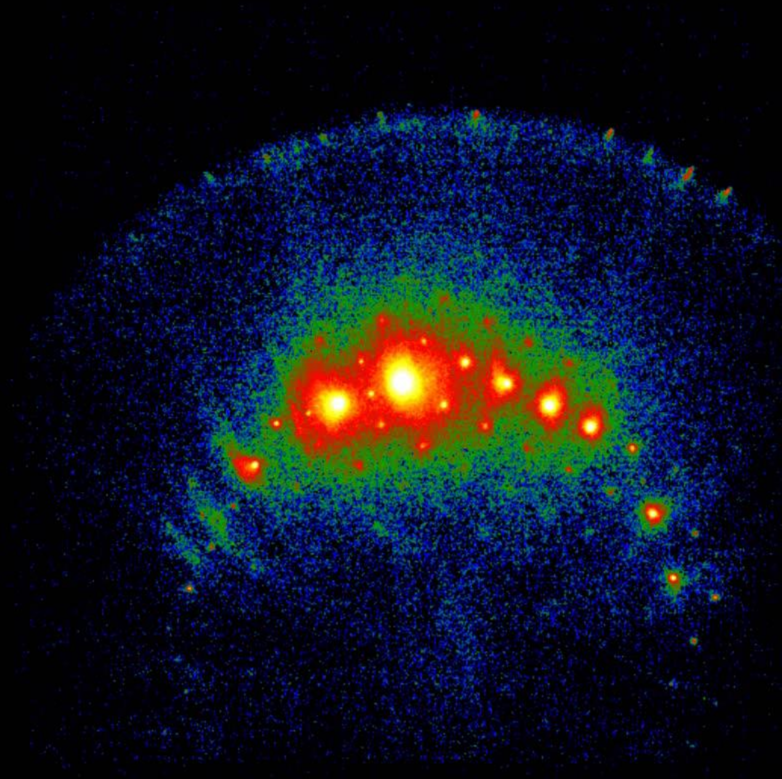

Sample: SrTiO3, not energy filtered, microscope: Zeis EM912, 120 kV

LARBED data acquisition by QED Plugin to DigitalMicrograph (HREM Research)

From PED => LARBED

Sample: Si (110), energy-filtered

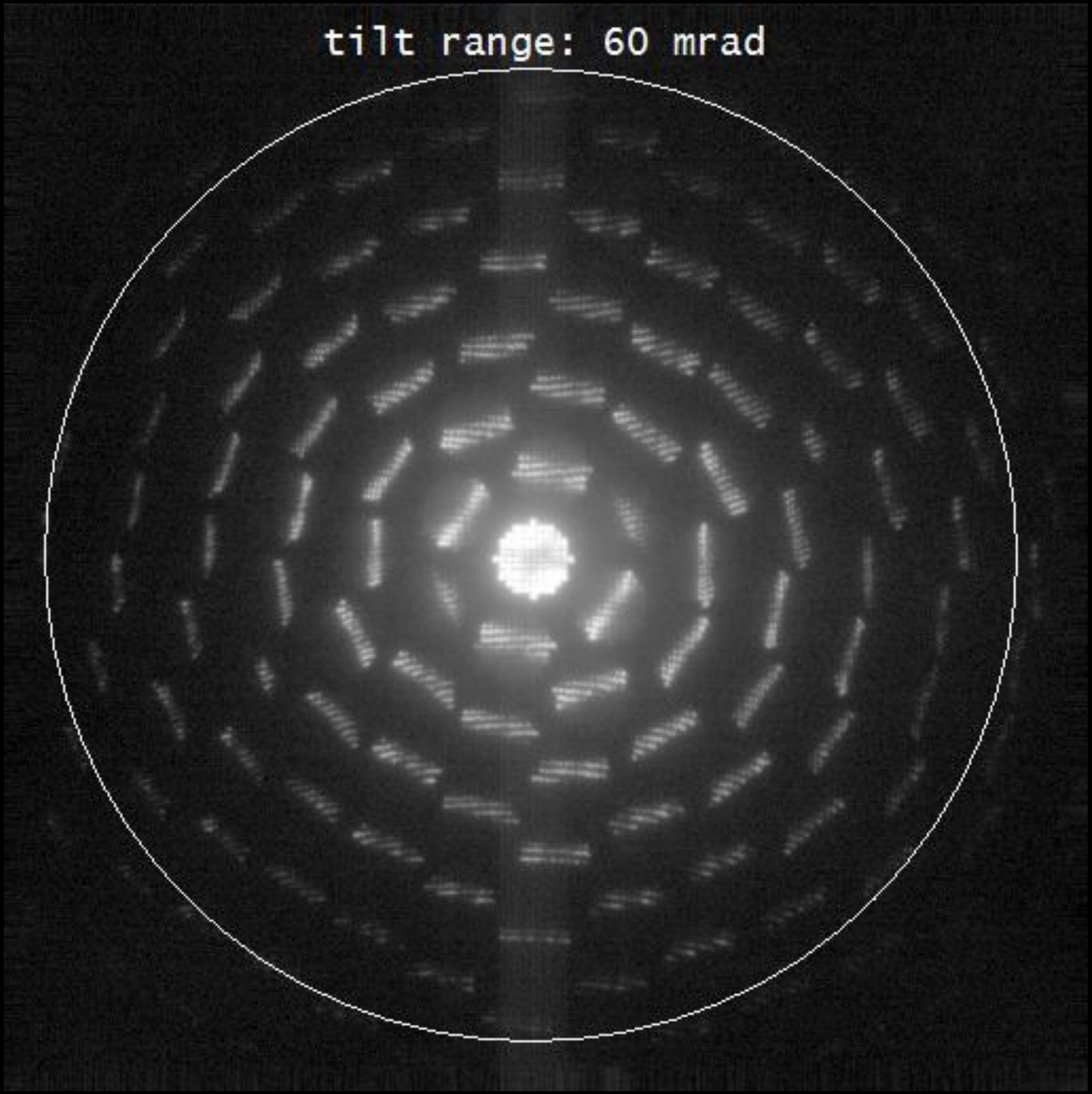

LARBED preserves the rocking curve information !

Extracting LARBED Discs from data stacks

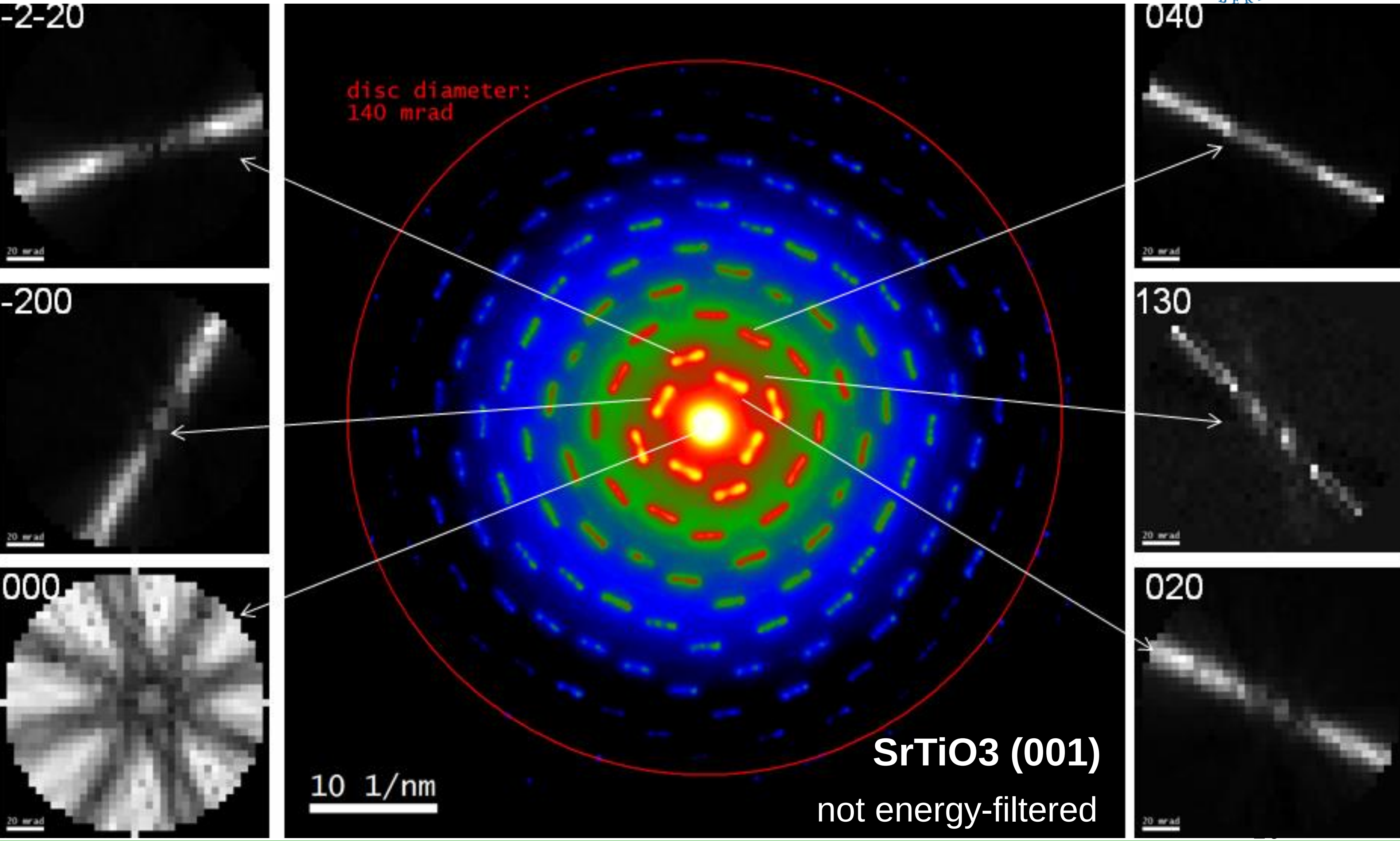

Each pixel within the discs is the integrated background-subtracted Bragg intensity

Correcting Ewald-Sphere Curvature & Separating Laue Zones

Extracted Zero-Order Laue Zone

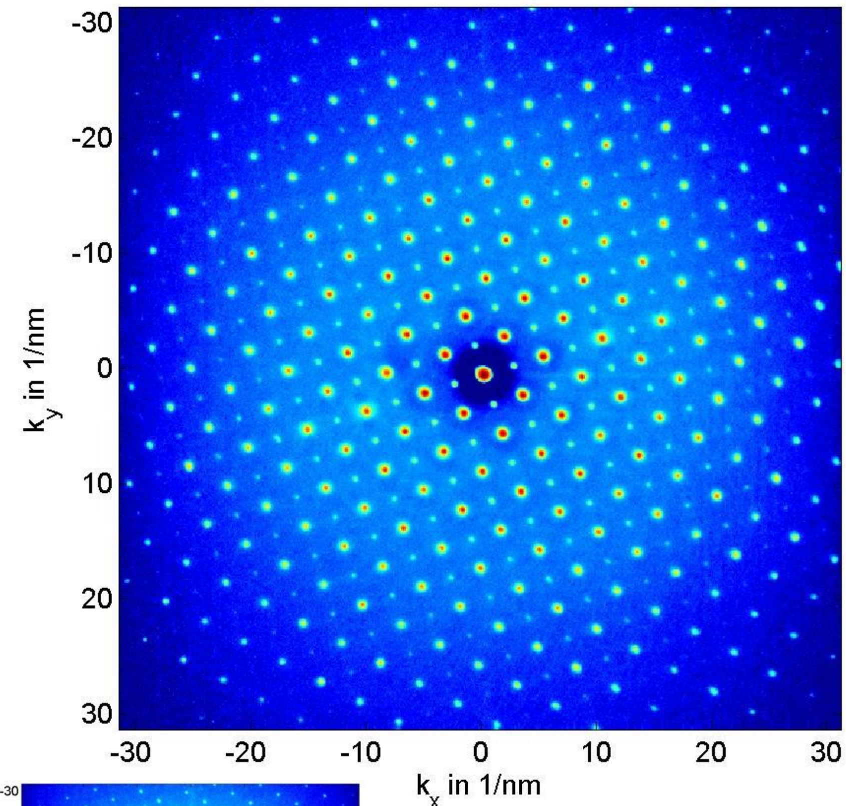

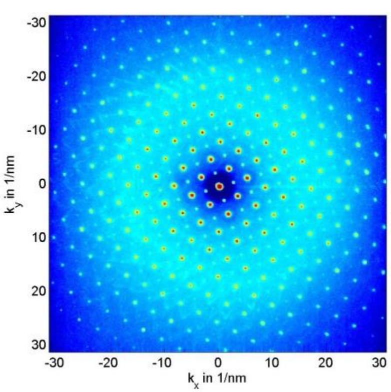

Sum of all frames

3D View

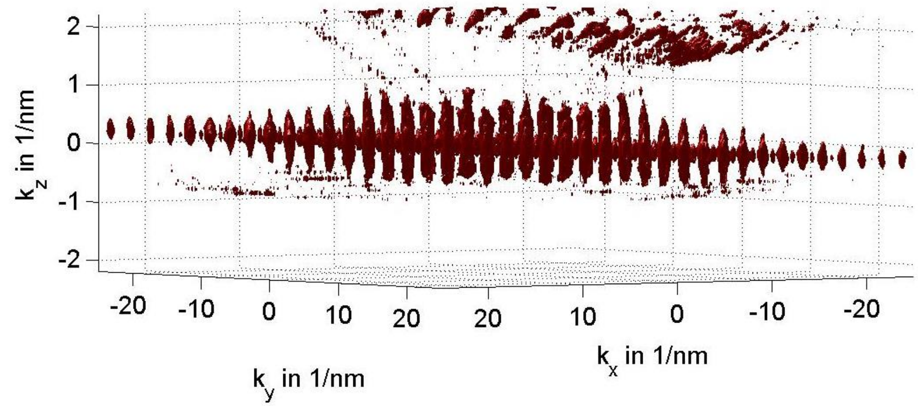

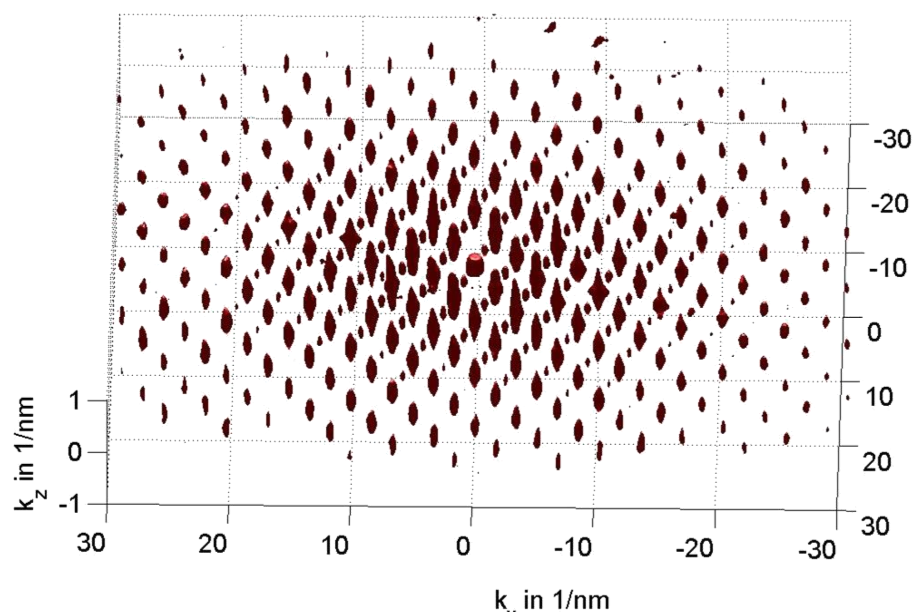


Feng Wang

Ab-initio Structure Factors Fitting to $SrTiO_3$ LARBED data

Experiment | *ab-initio* Fit | Difference

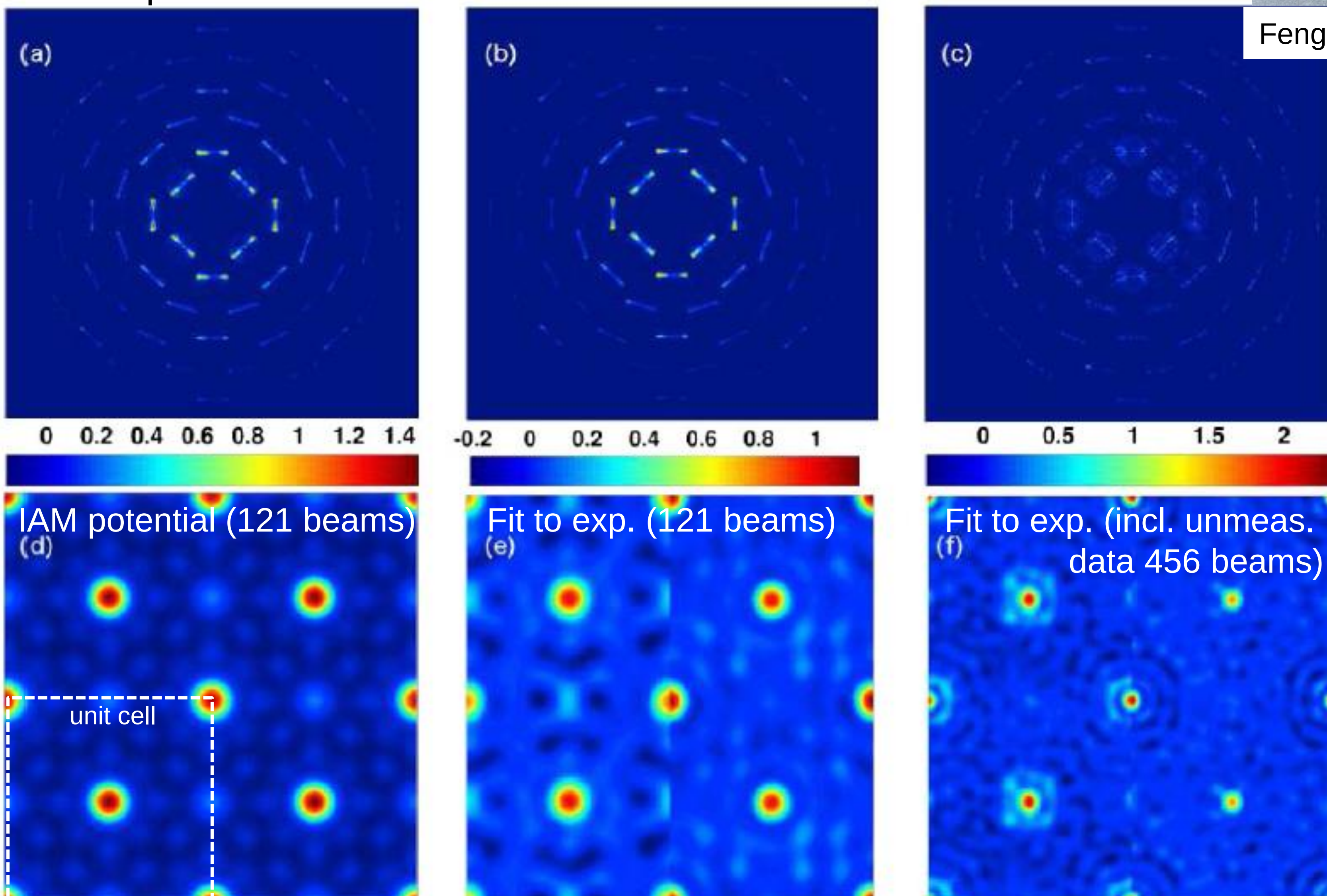

F. Wang, et al. Phys. Rev. Lett. 117 (2016) 015501

LARBED on a 60 nm MgO cube

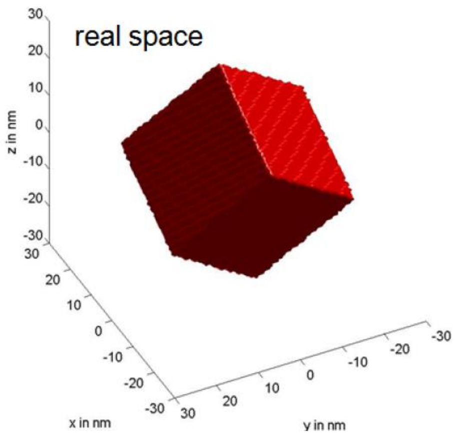

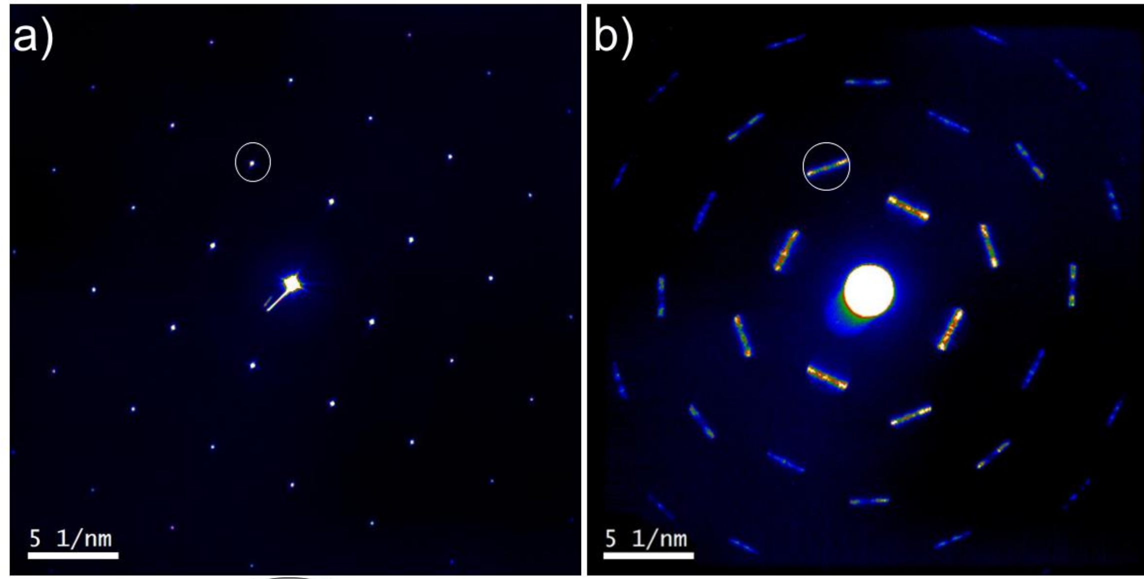

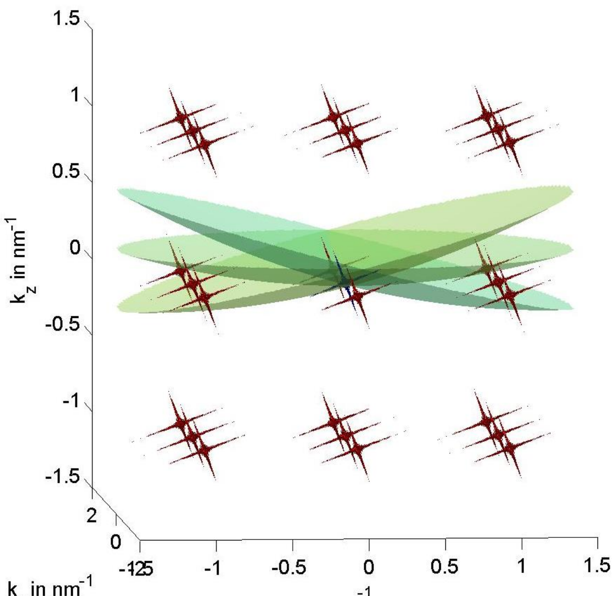

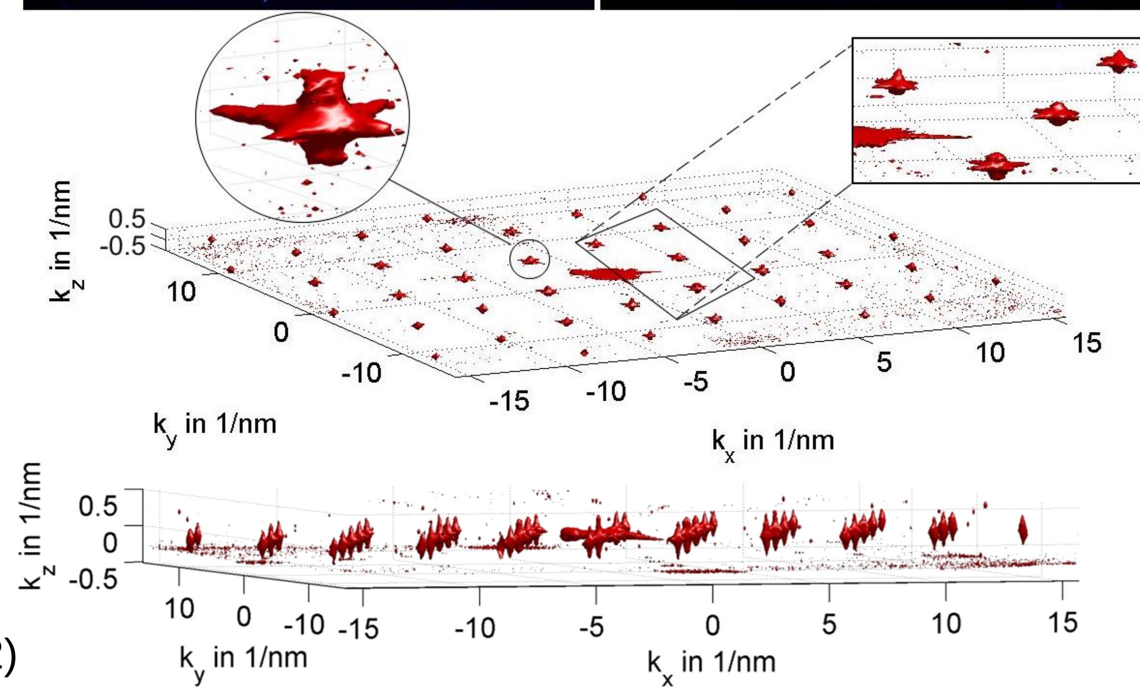

C.T. Koch et al. Microsc. Anal. (2012)

$K_2O \cdot 7Nb_5O_2$ (‘KNbO’) (001)

Space group P4/mbm (No. 127), a=b=27.5Å, c=3.94 Å

Only in the (001) orientation the HOLZ planes are well separated!

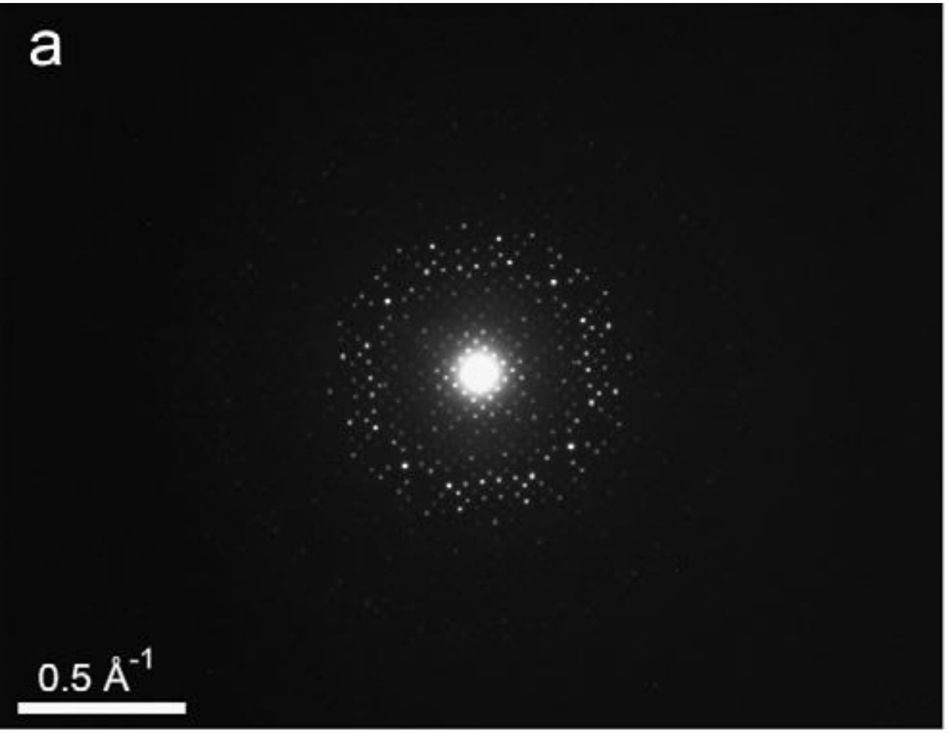

SAED of $K_2O \cdot 7Nb_2O_5$

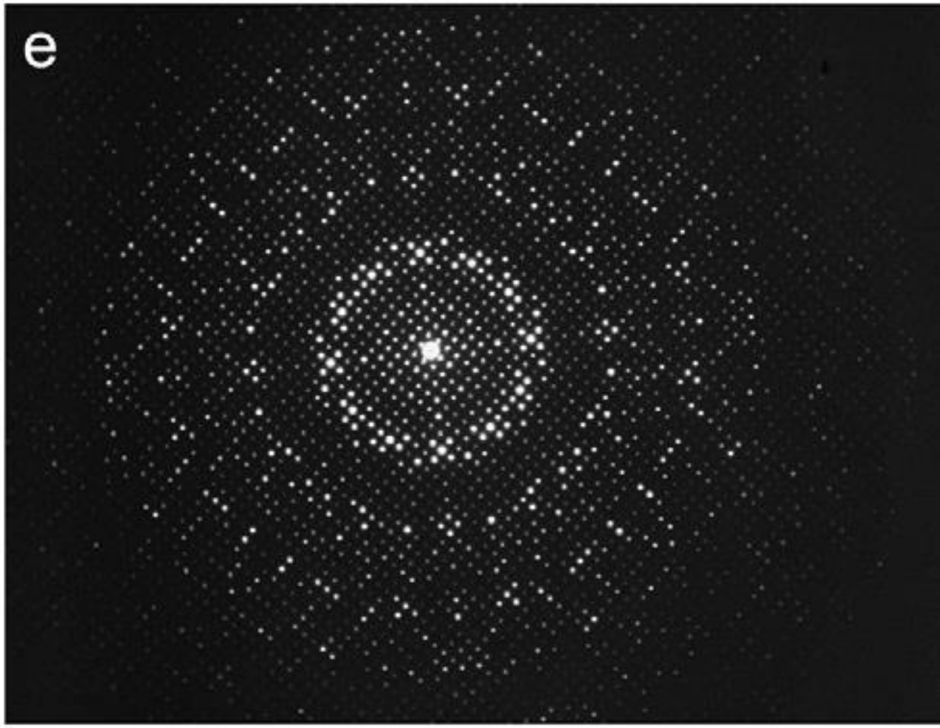

max-PED pattern

Images from D. Zhang et al, Ultramicroscopy 111 (2010) 47–55

$K_2O{\cdot}7Nb_5O_2$ (arbitrary orientation)

Single Diffraction Pattern

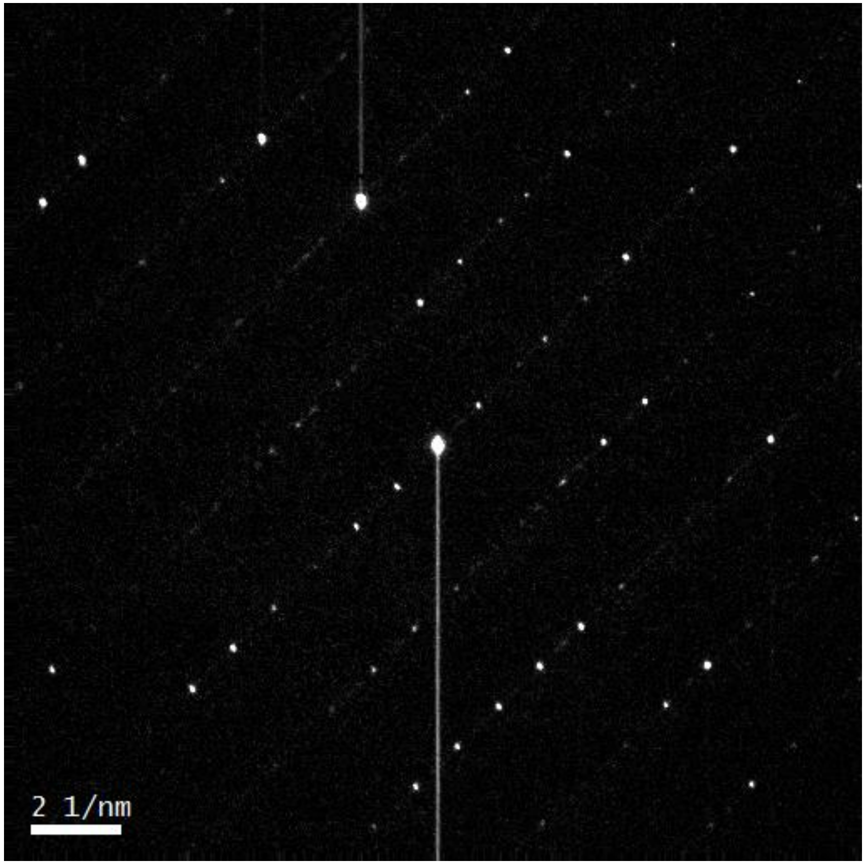

Integrated PED Pattern
(LARBED with full scan compensation)

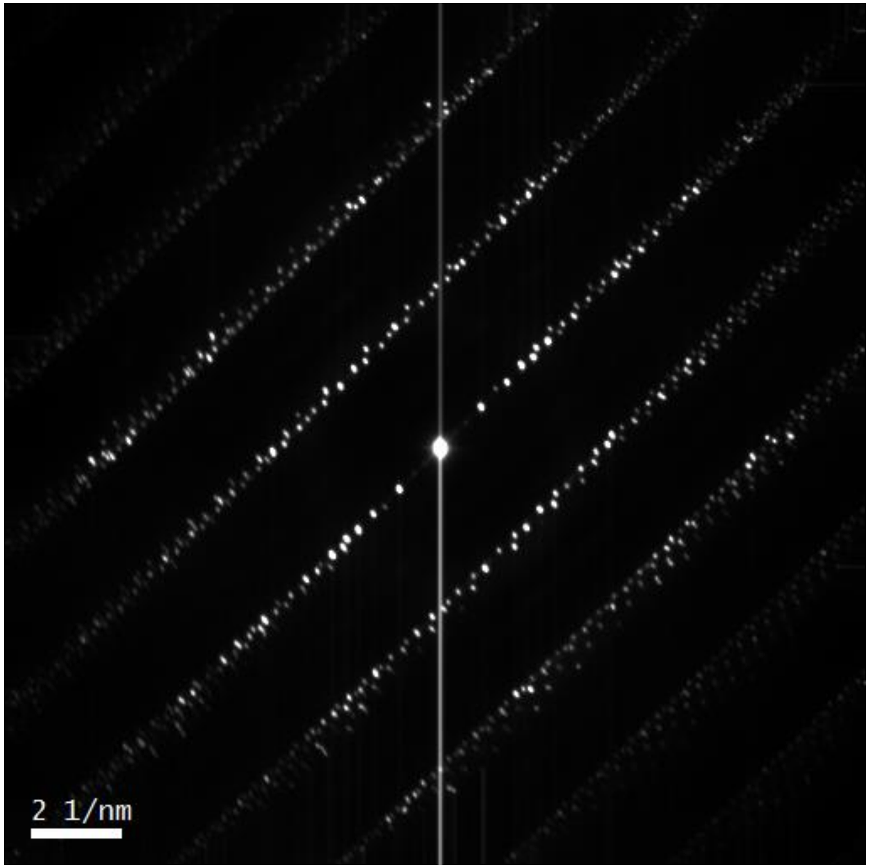

Energy-filtered diffraction patterns recorded on Zeiss SESAM using a Gatan UltraScan 1000 CCD Camera

Sample kindly provided by D. Zhang & S. Hovmöller

Extracting DF-LACBED Discs

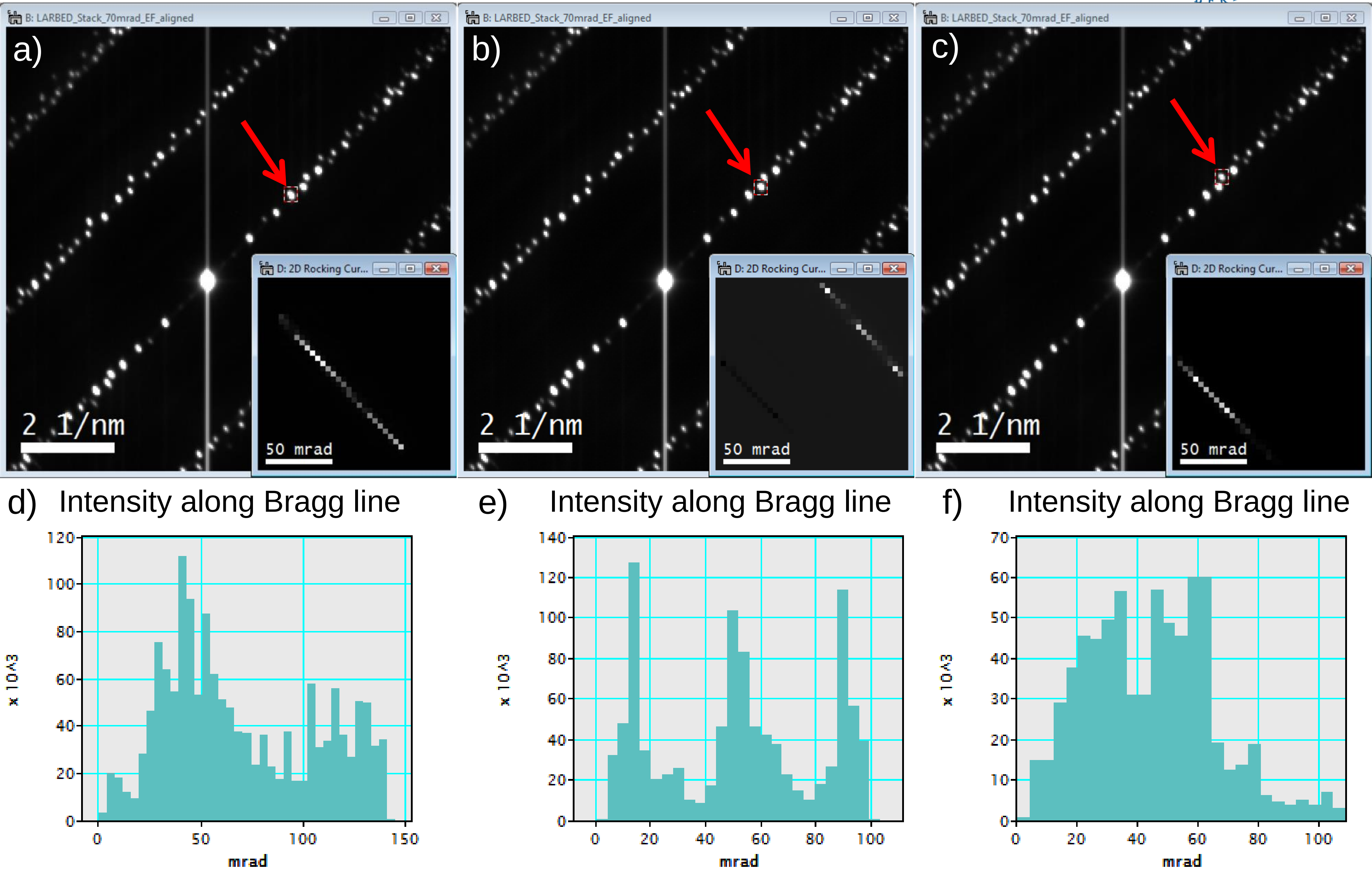

Bragg-lines = equal positions in 3D k-space

Large intensity fluctuations along Bragg lines

$\Rightarrow$The more of it you collect the better

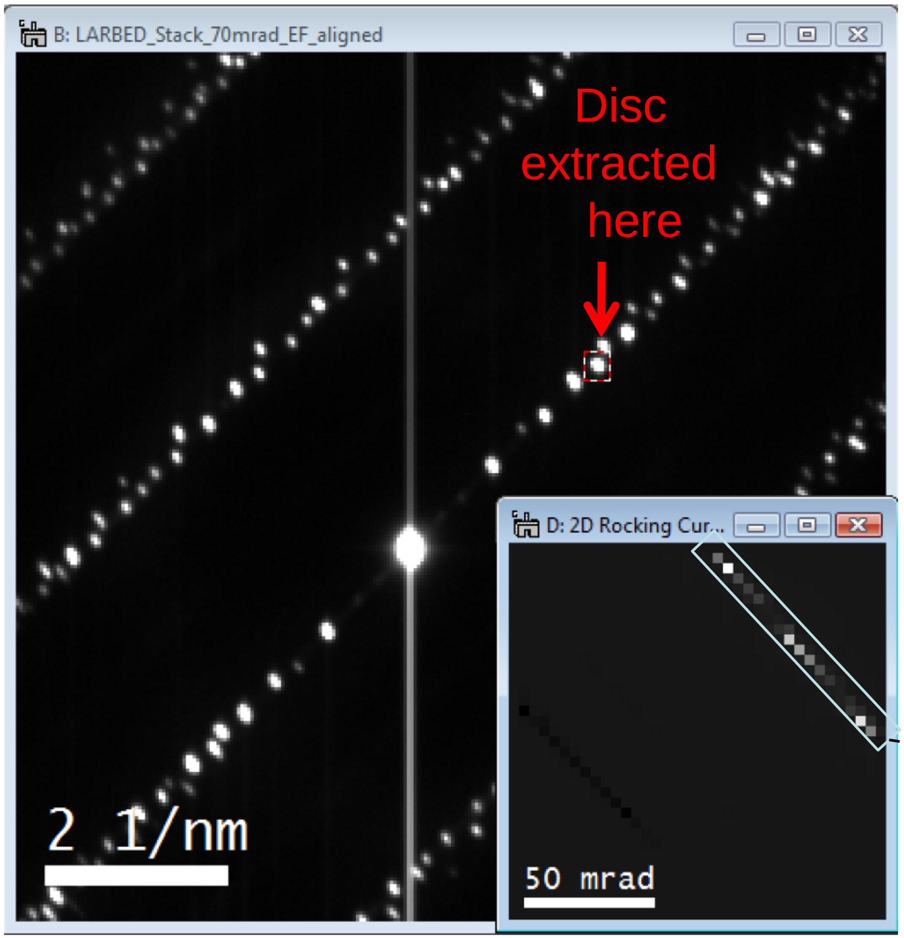

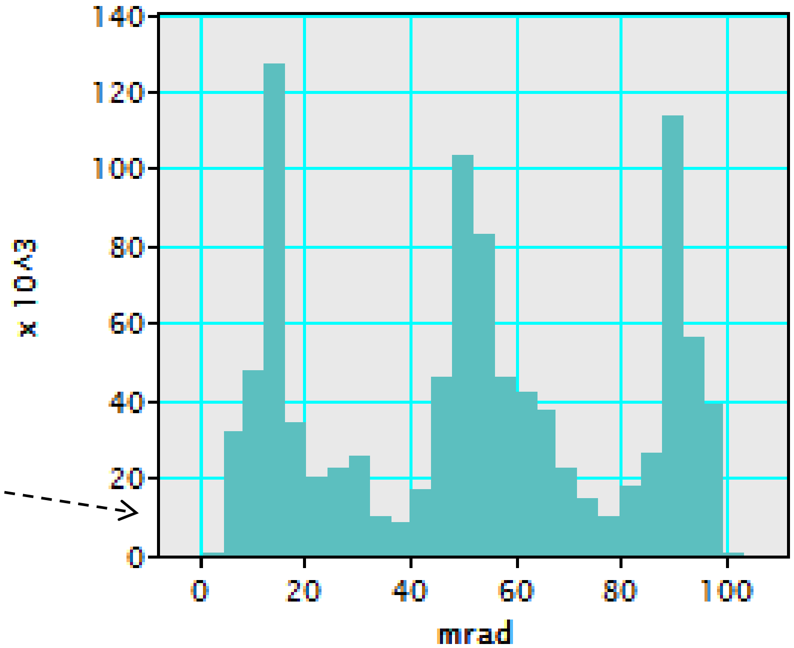

Reconstruction of 3D k-Space

Each voxel in this 3D k-space is the intensity averaged along the corresponding Bragg line

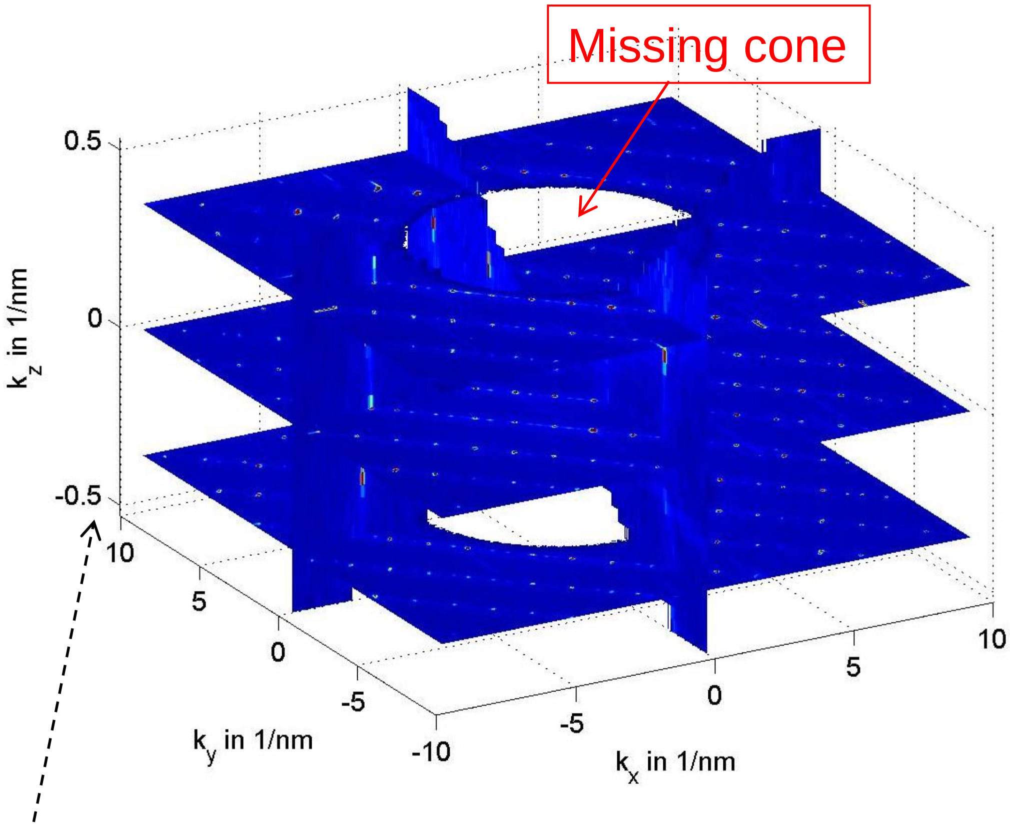

k_z-axis expanded

Central (horizontal) slice of reconstructed volume

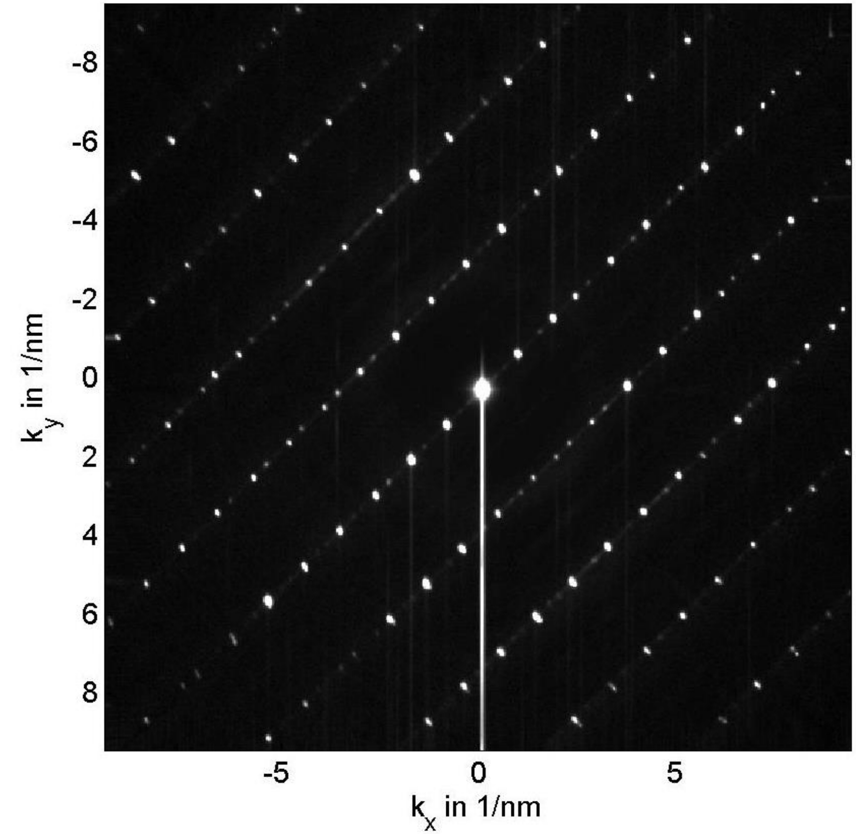

3D k-Space Integrating Electron Diffraction

Reconstructed 3DBLED Volume

Vertical cuts through reciprocal space

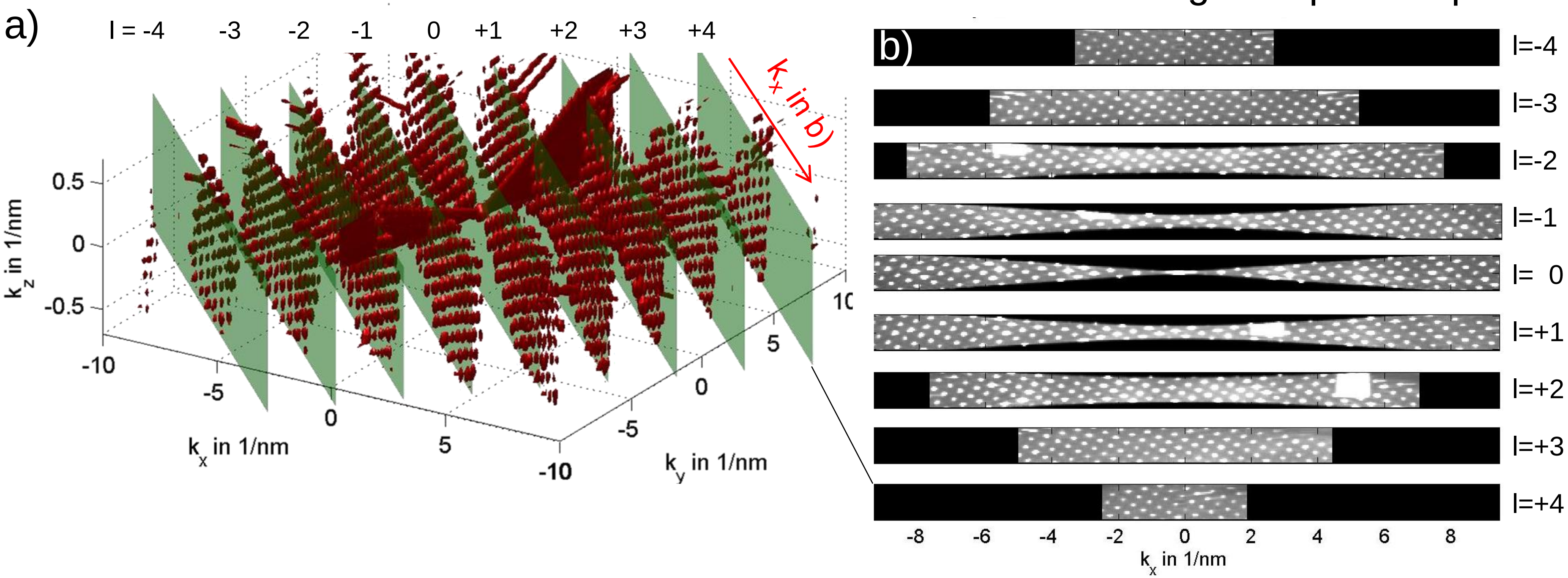

z-axis expanded x 5

Contrast adjusted
to show all diffraction spots
(equal scale along x and z)

Each voxel in this 3D space represents the average along the corresponding Bragg line

3D Reconstruction of k-Space for Complex Structure

Reconstructed 3D k-space Volume
from experimental LARBED data

z-axis expanded x 5

Sample: $K_2O{\cdot}7Nb_5O_2$
(a=b=2.9 nm, c = 0.39 nm)

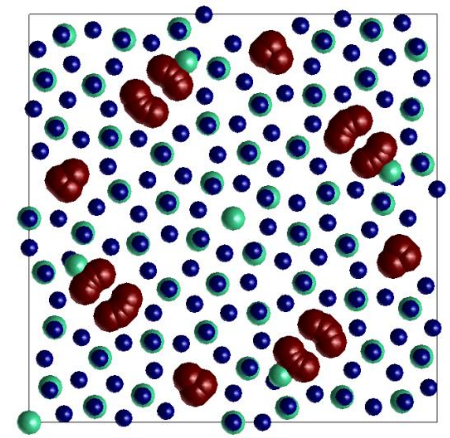

Rocking curves for each spot in 3D k-space

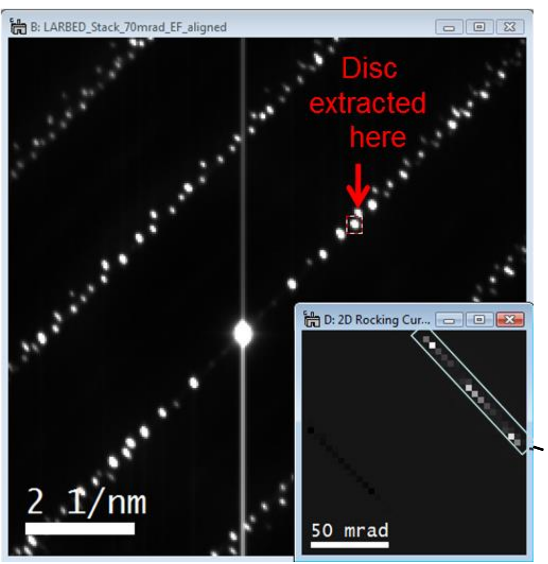

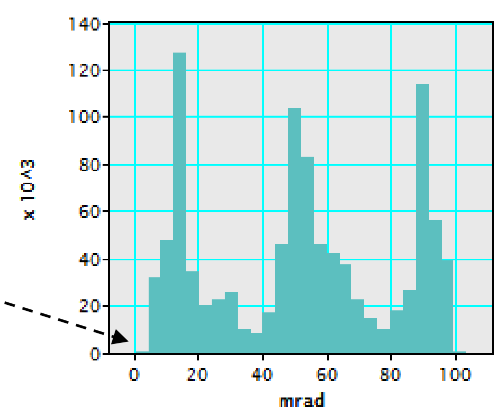

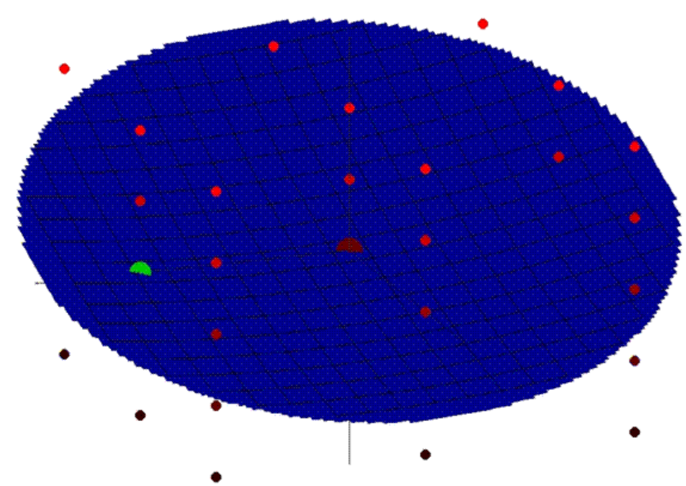

Extending CBED disc sizes

CBED pattern of Si near (110)

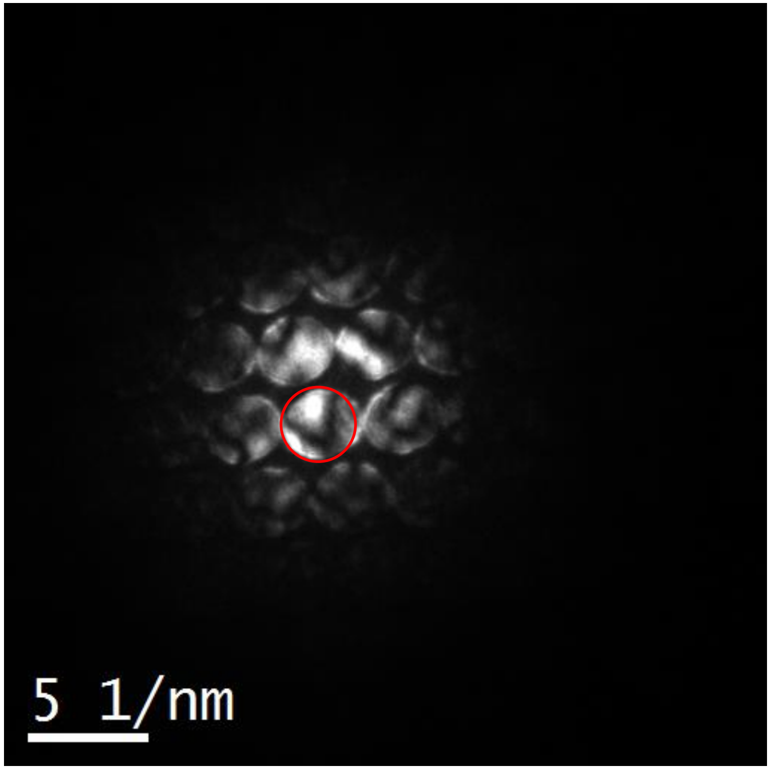

Where is the zone axis center?

Extended (000) disc

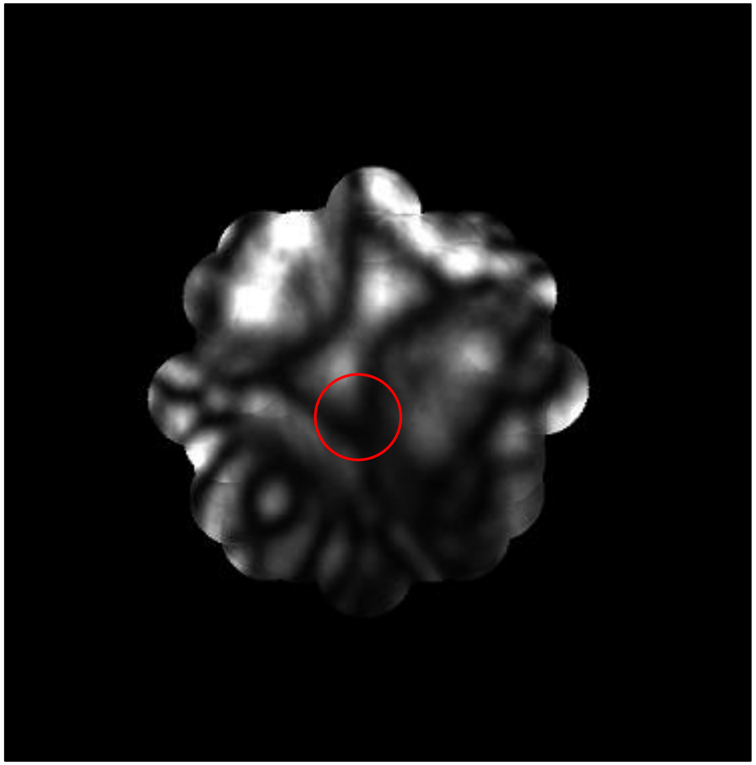

Zone axis center can be localized!
Symmetry becomes obvious

Large-angle rocking convergent beam electron diffraction

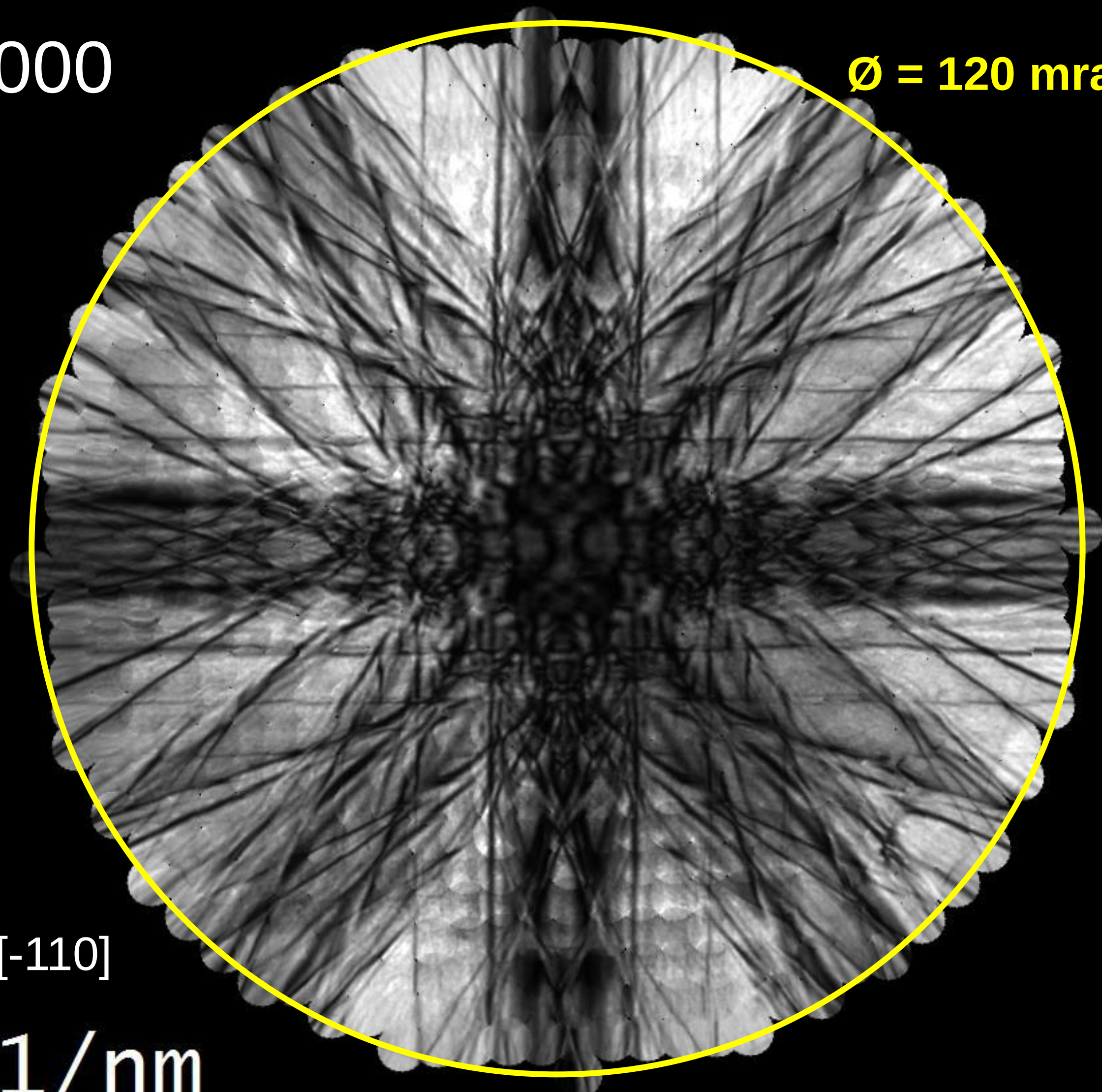

$SrTiO_3$ [-110]

20 1/nm

Acquisition by QED Plugin to DM (HREM Research)

TEM: SESAM (200 kV), zero-loss filtered

See also: R. Beanland et al. Acta Cryst. (2013). A69, 427

Outline

1. Motivation
2. Precession Electron Diffraction (PED)
3. Aberration compensation
4. Large-Angle Rocking-Beam Electron Diffraction (LARBED)
5. Strain Mapping

Strained Silicon

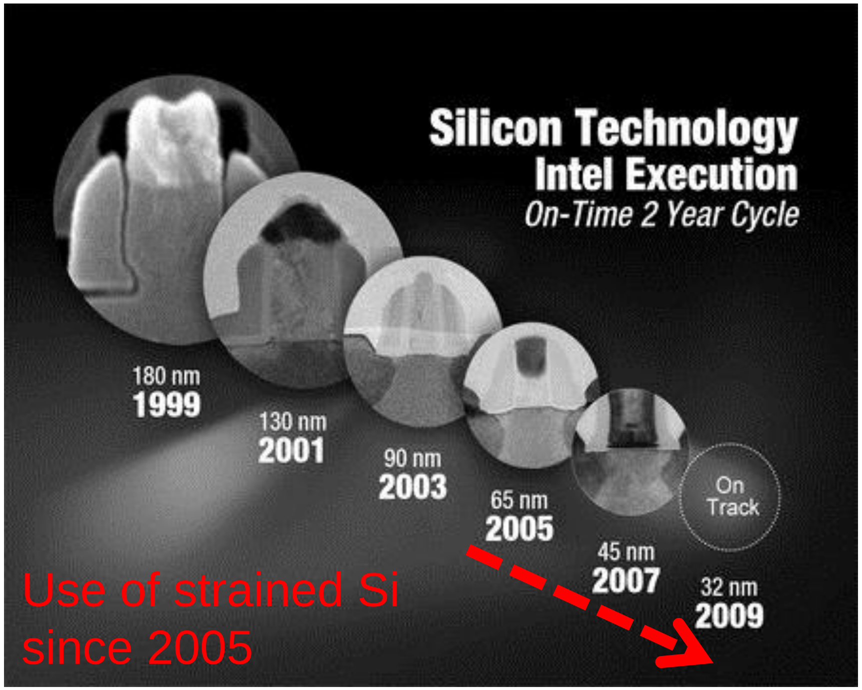

Semiconductor industry

- 2009: $260 Billion market
- ≈ 10% of world GDP (incl. electronic systems & services)

unstrained lattice

strained lattice

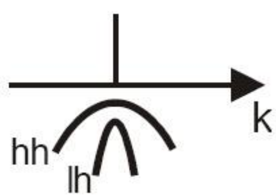

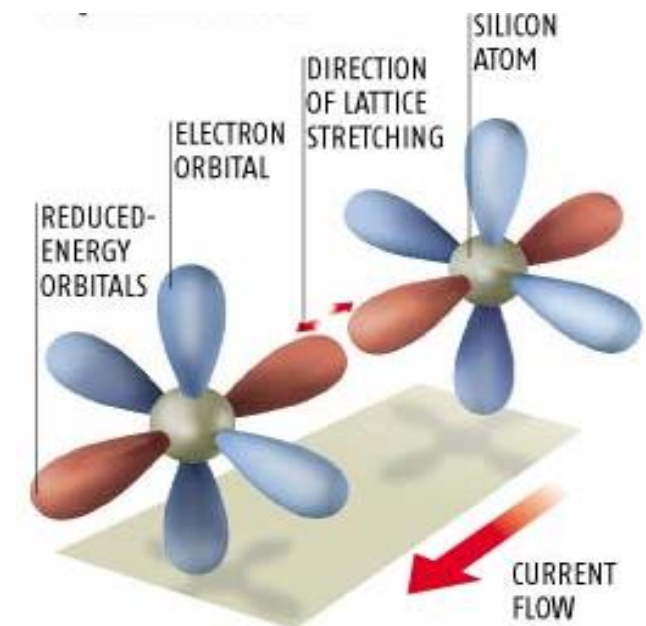

$m^* \sim 1/(d^2E/dk^2) \sim 1/\mu$

band curvature => reduction in effective mass m*
band splitting => less inter-valley scattering

Strain Mapping by Nanodiffraction

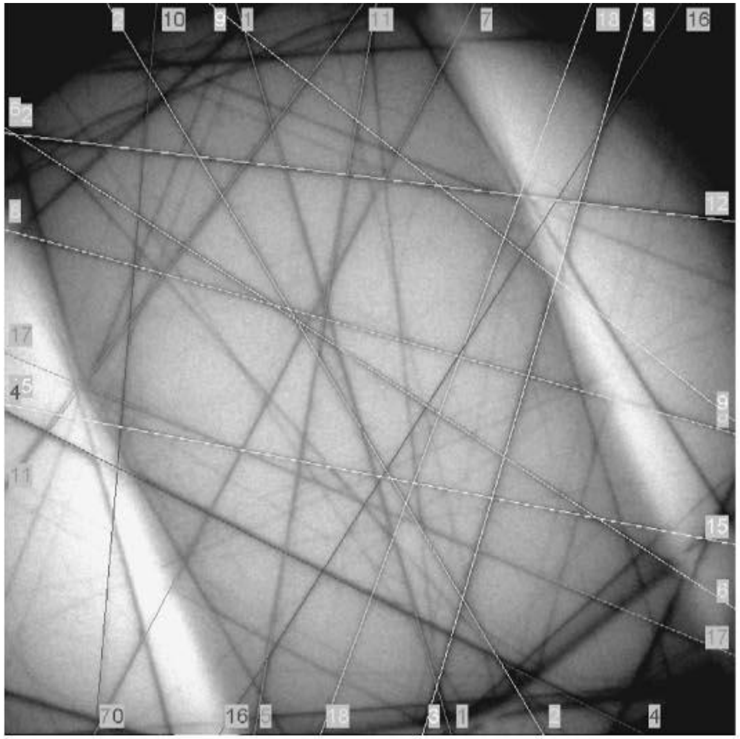

Holz line fitting for single crystal silicon <230>

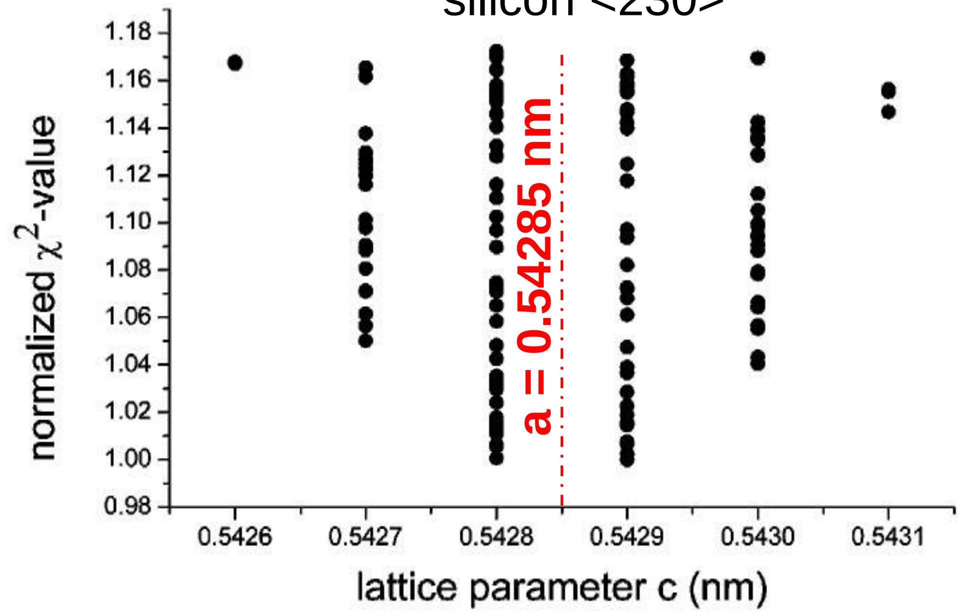

FLASH memory cell

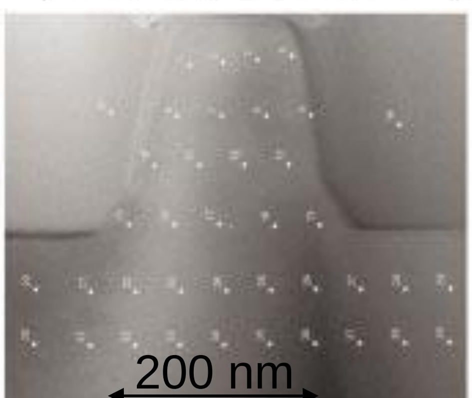

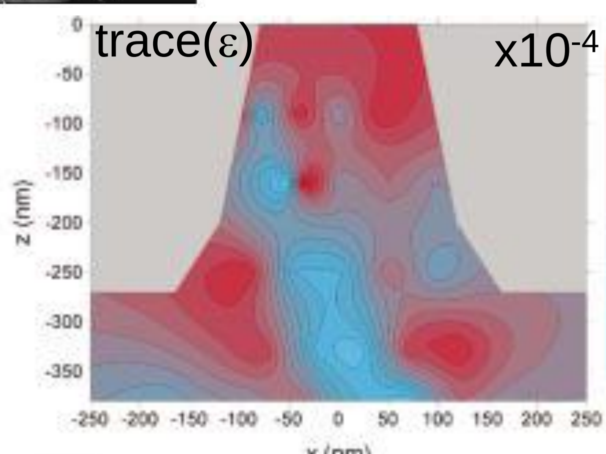

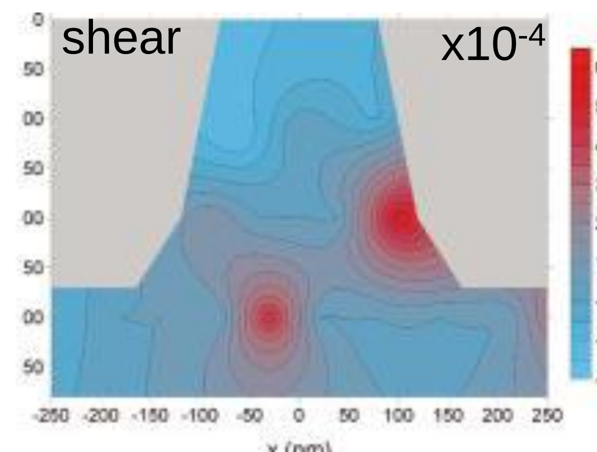

A. Armigliato et al., APL **82** (2003) 2172

PED helps in strain mapping (averages over orientations)

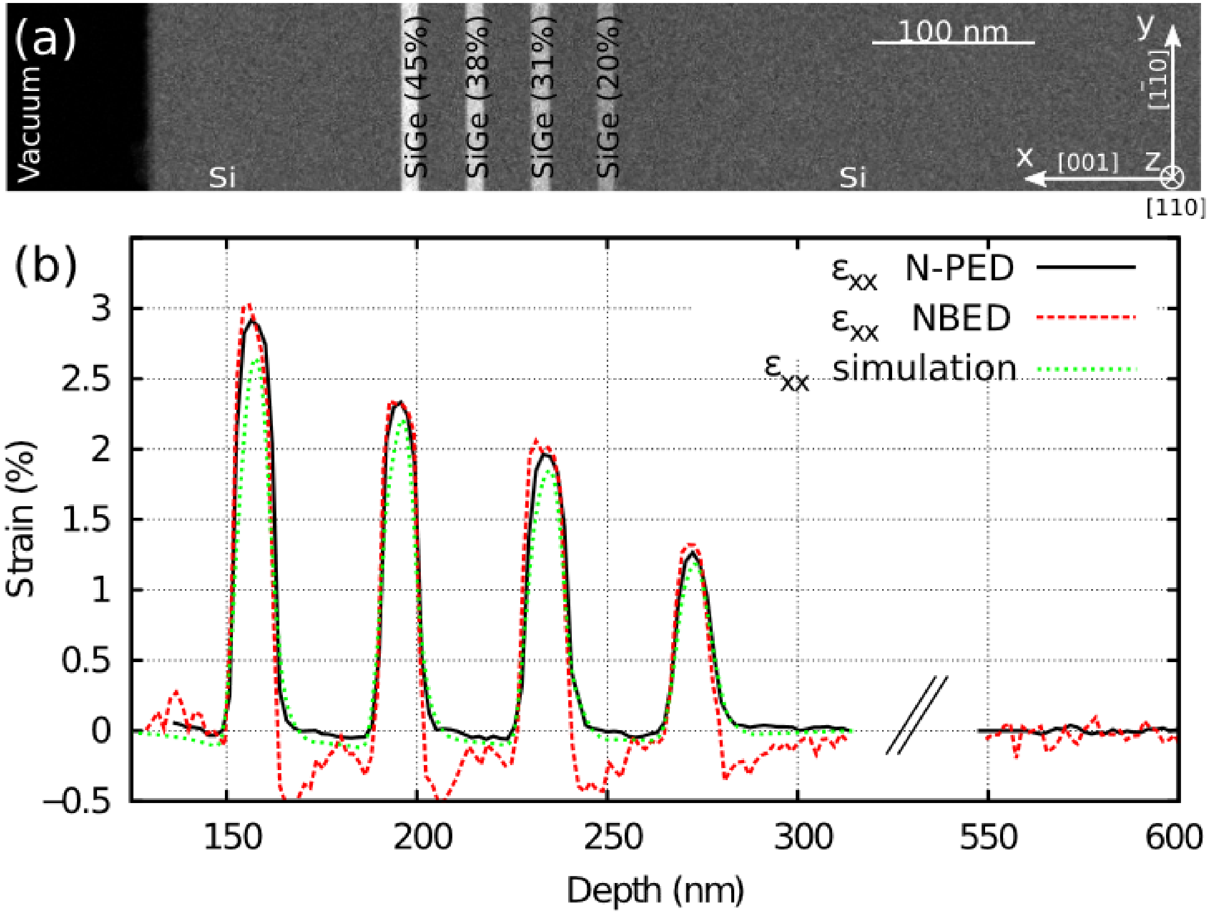

FIG. 2. (a) HAADF-STEM image of the observed sample composed of four SiGe layers deposited on a (001) silicon substrate. (b) ε_{xx} strain profiles obtained from N-PED, NBED and simulations.

J.L. Rouviere et al. Appl. Phys. Lett. 103 (2013) 241913

CBED: Problems @ High Resolution

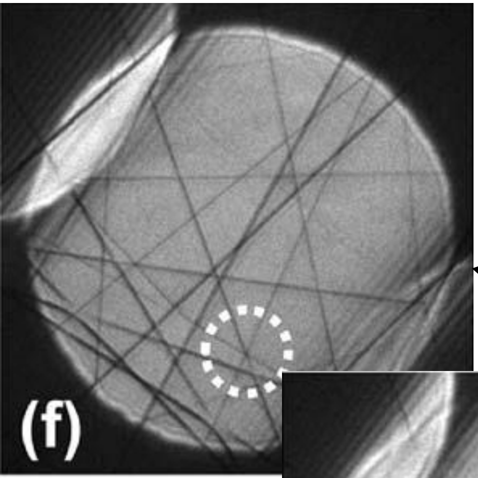

25 nm
below gate

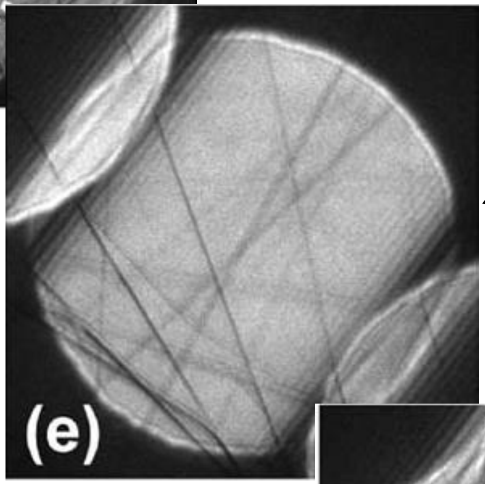

55 nm
below gate

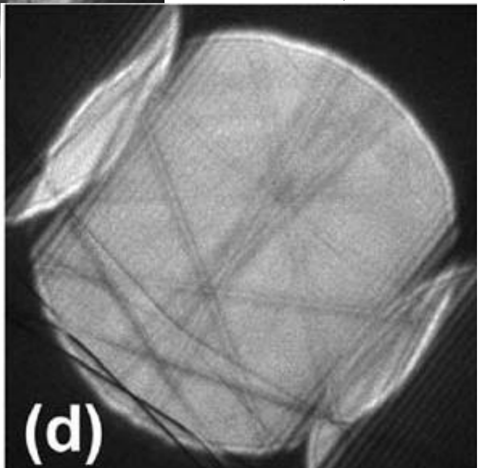

100 nm below gate

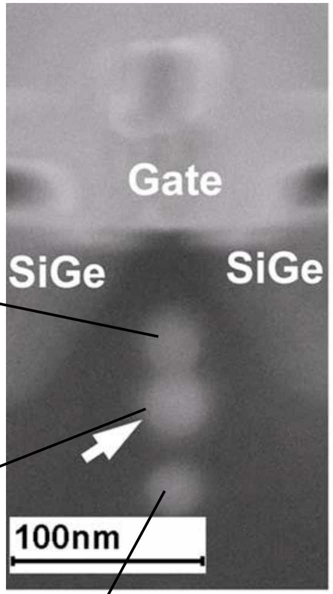

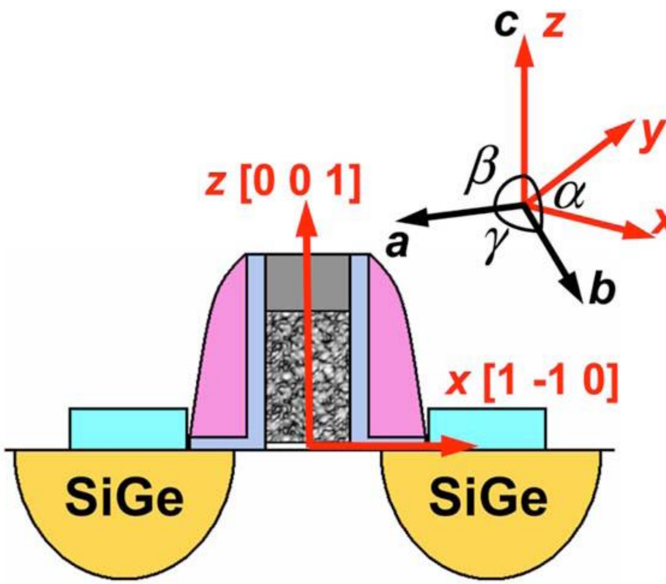

P. Zhang, APL **89** (2006) 161907

Process-induced Strain

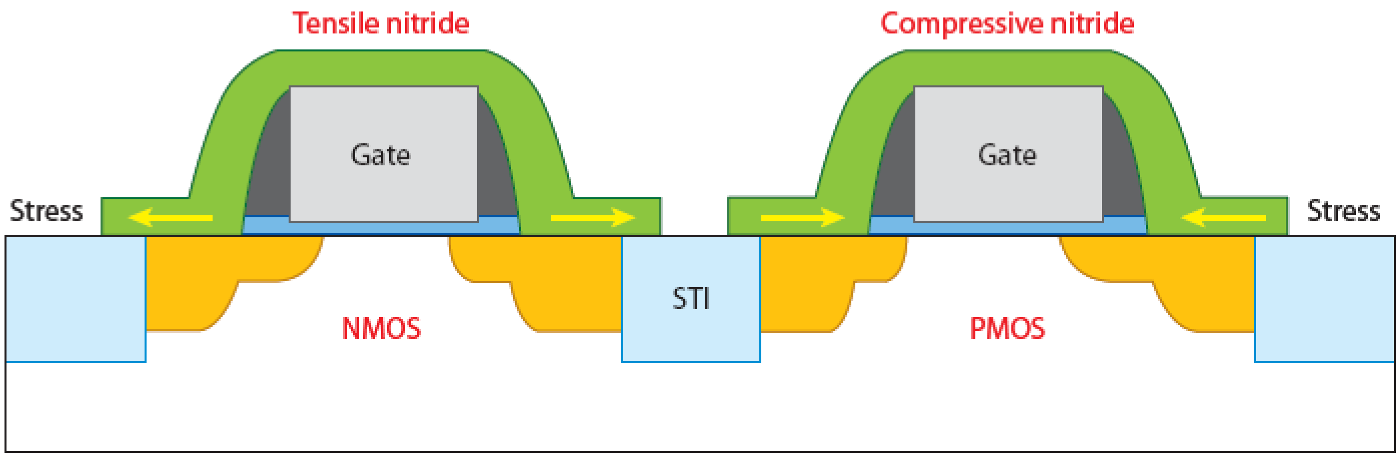

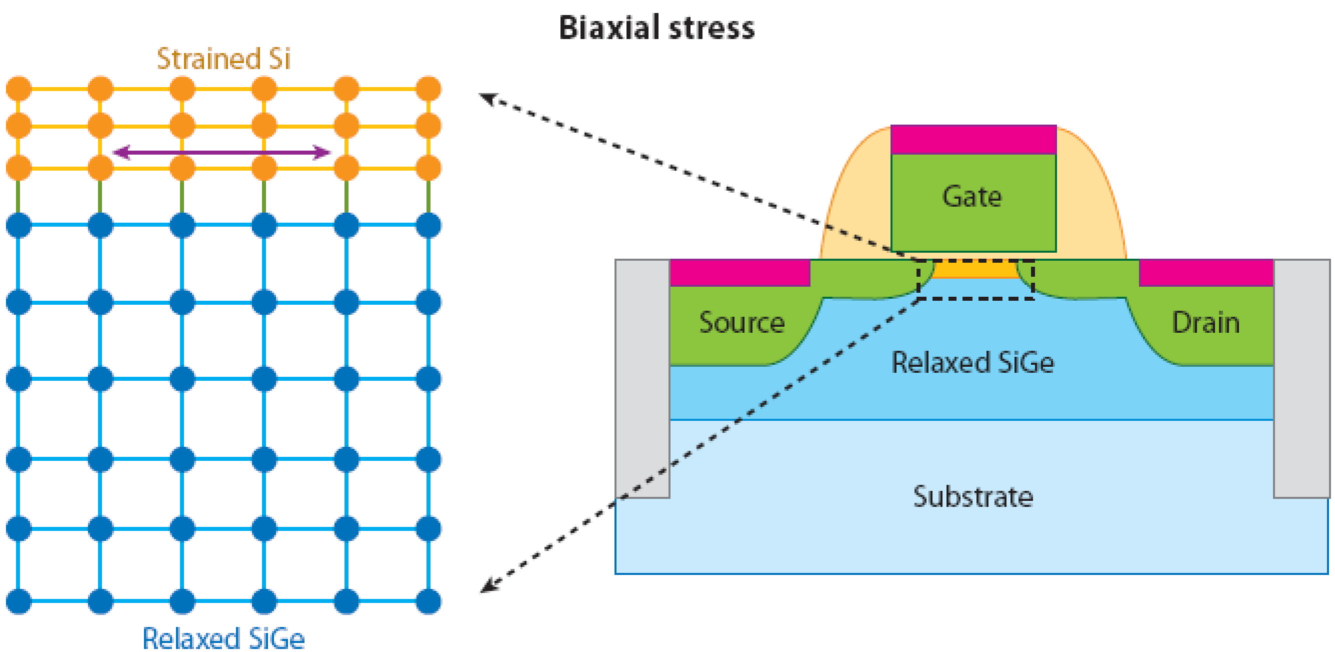

M. Chu et al, Annu. Rev. Mater. Res. **39** (2009) 203–29

Strain in thin films

Si – $Si_{0.7}Ge_{0.3}$ – Si sandwich

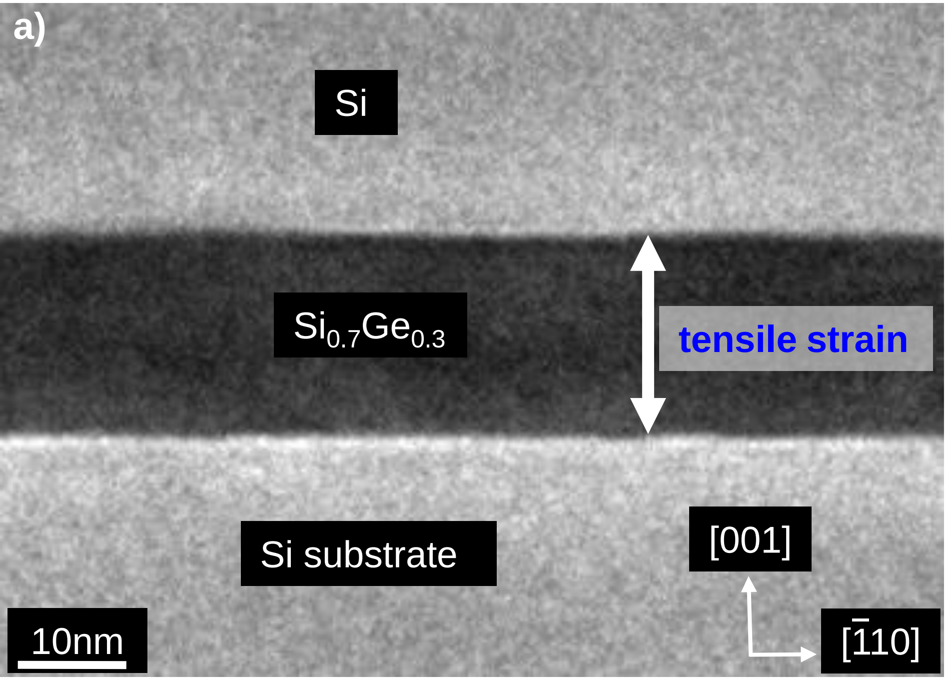

Sample provided by
E. Kasper, University of Stuttgart

CMOS transistor structure

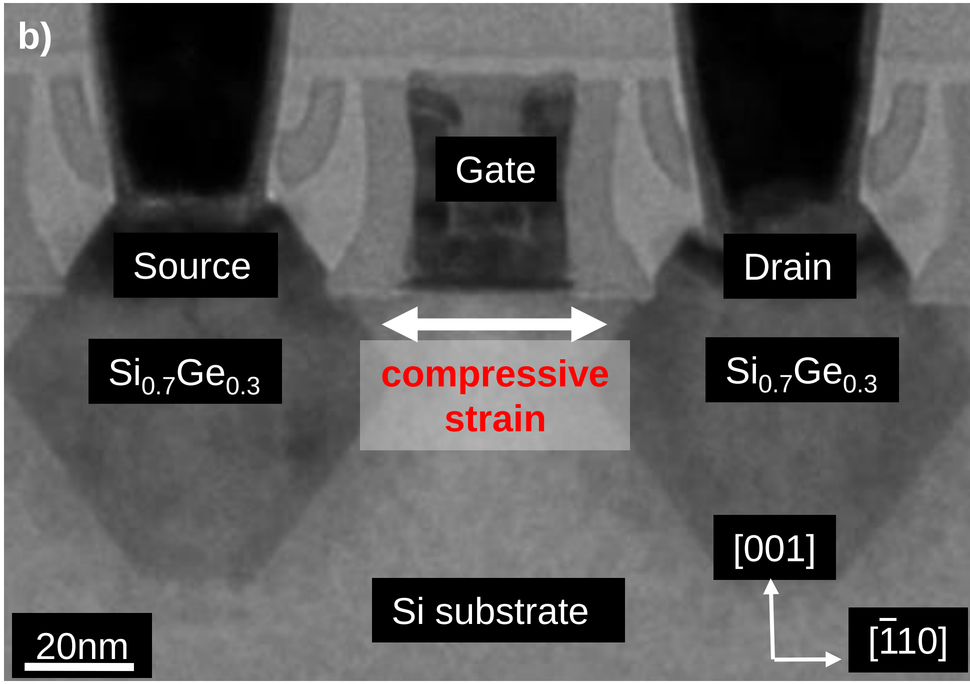

Sample:
Commercial processor (45 nm technology)

Strain Mapping by HRTEM

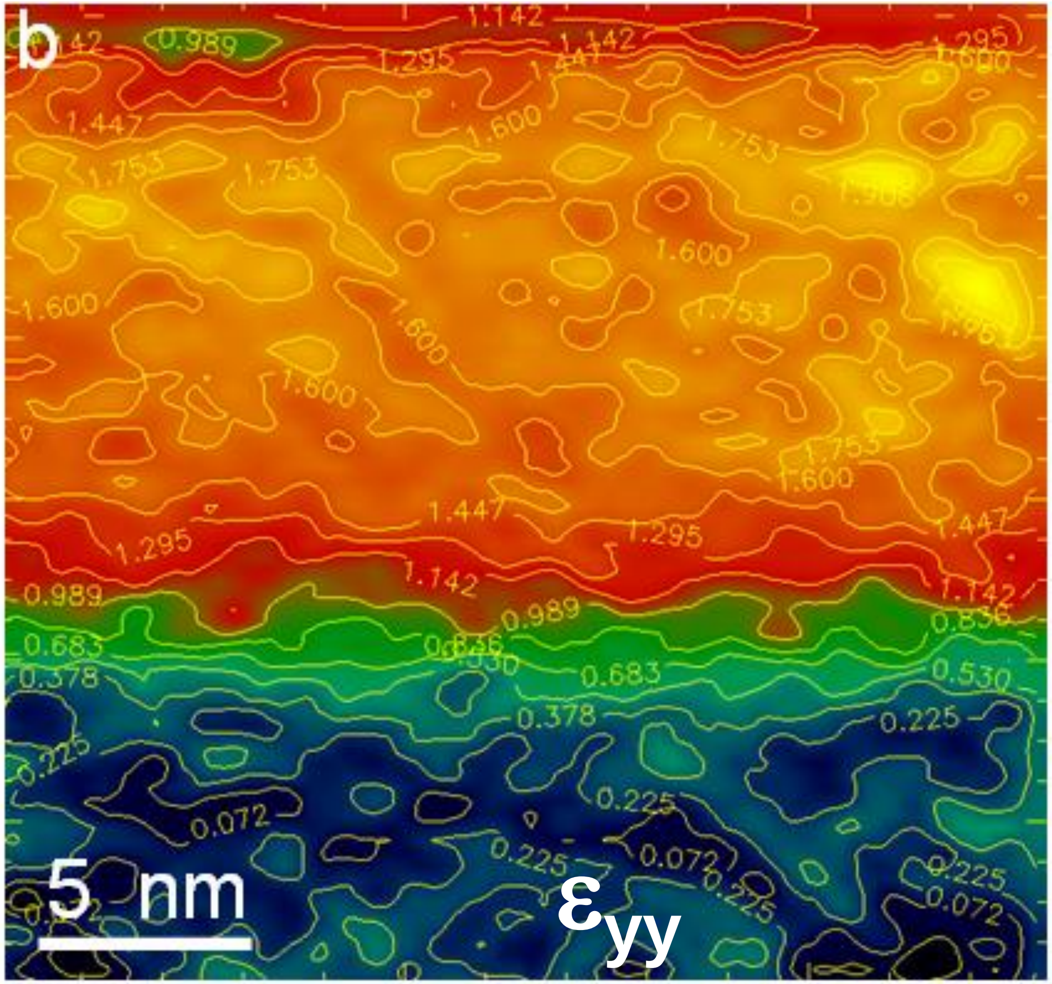

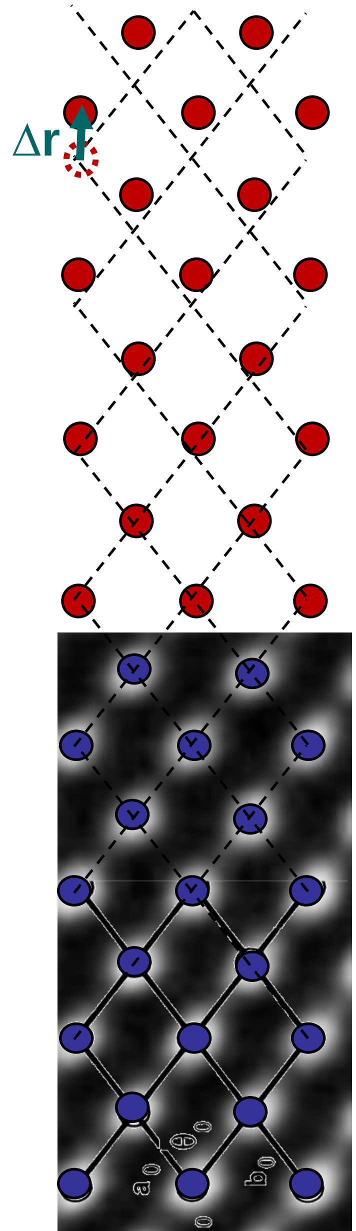

Strain tensor:

$$\varepsilon_{ij} = \frac{\partial \Delta r_i}{\partial j}$$

K. Du, et al, J. Mater. Sci. Technol. **18** (2001) 135
V.B. Ozdol, et al, Microscopy Conf. 2009, Graz

Dark-Field Inline Holography

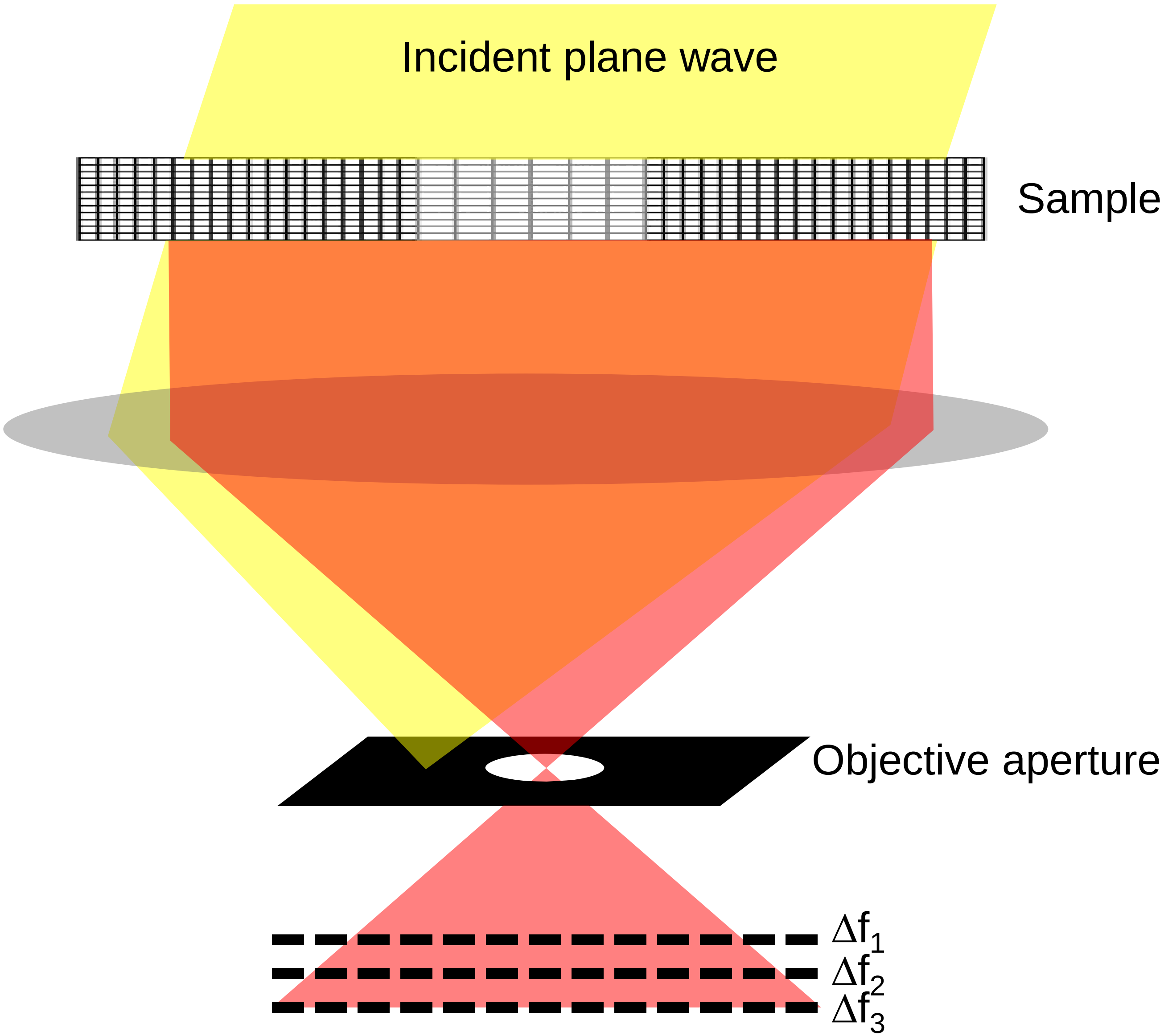

Dark-field Inline Holography

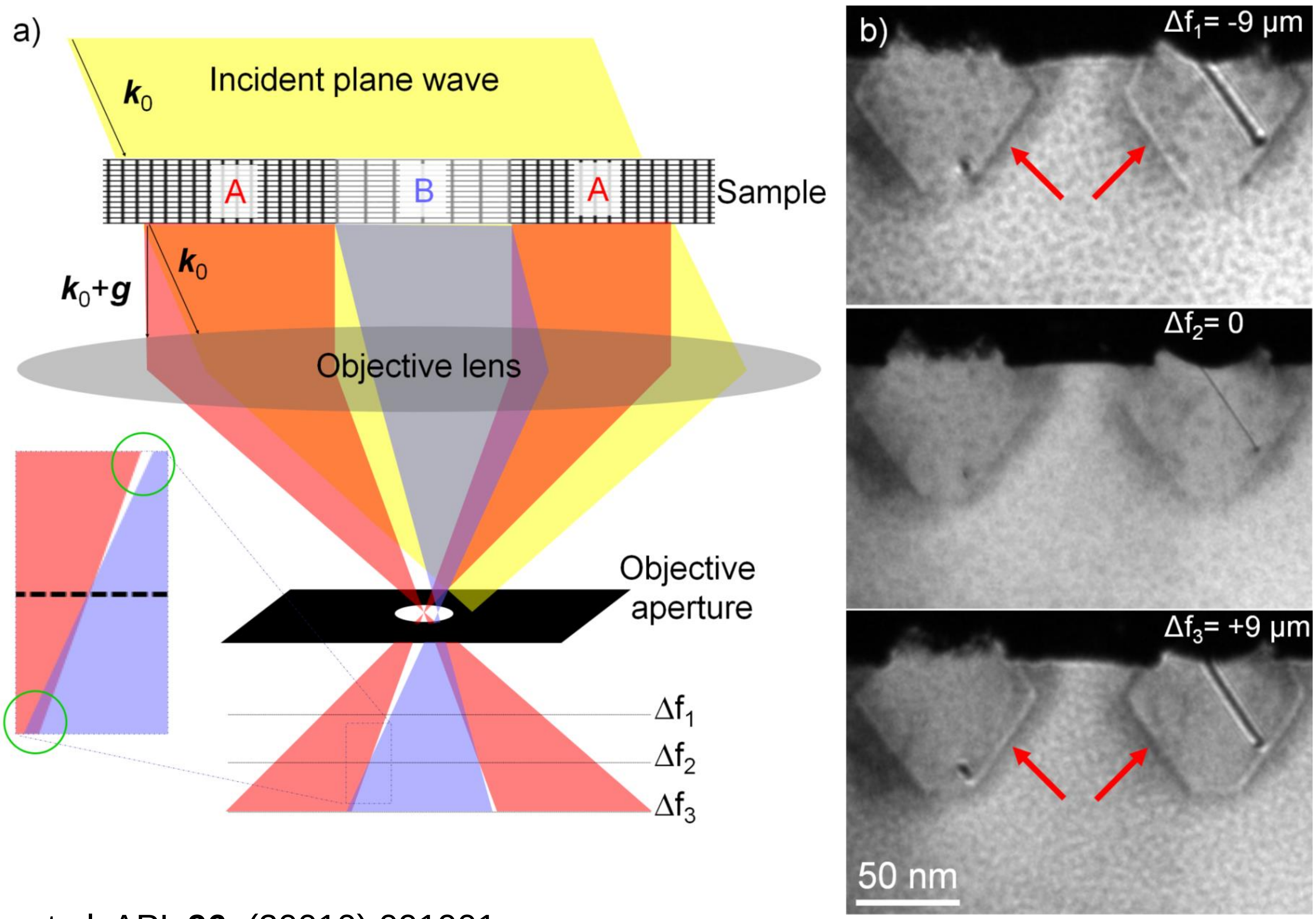

C.T. Koch, et al. APL **96,** (20010) 091901

Comparison of DF-Holography Strain Mapping Techniques

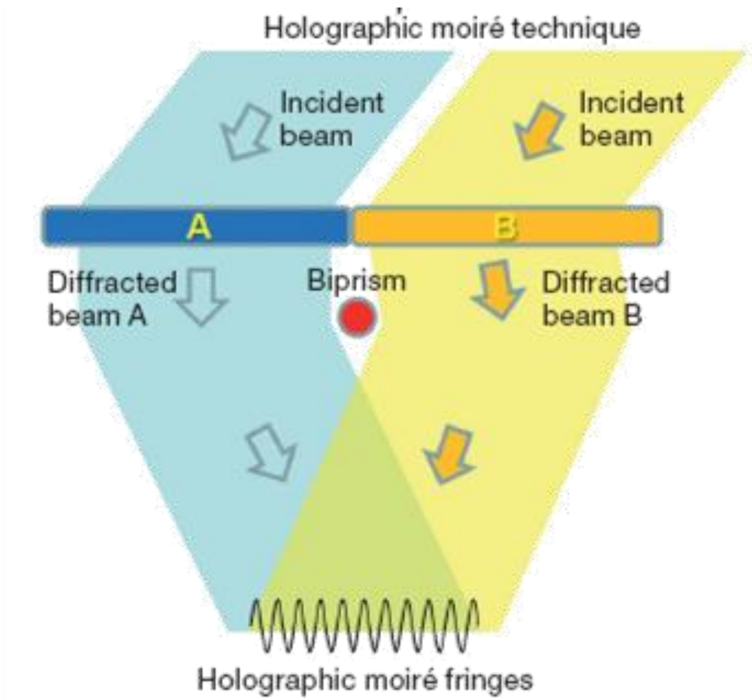

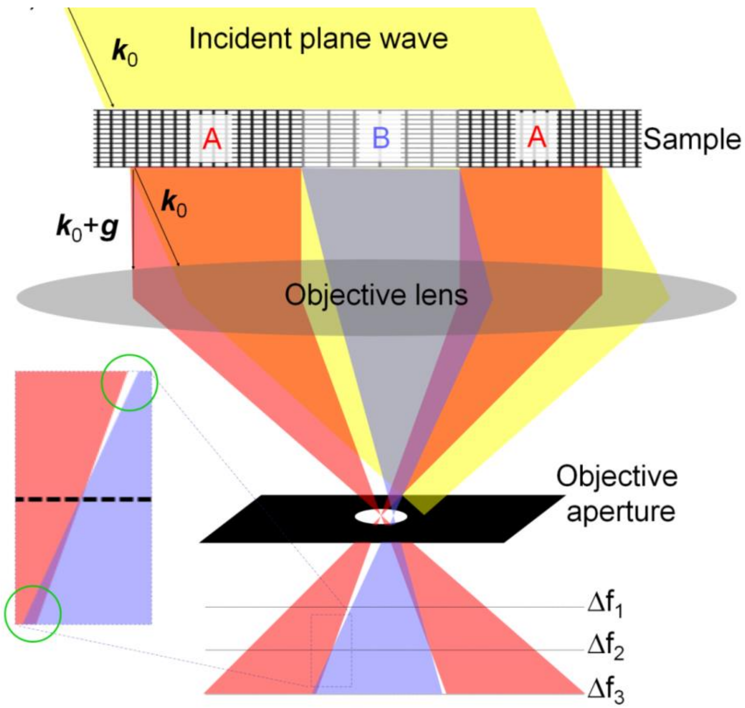

- Need reference area of perfect crystal
- Needs high spatial coherence

- No need for a reference area
- Works also with low spatial coherence

M. Hytch et al., Nature **453** (2008)

C.T. Koch et al., APL **96** (2010)

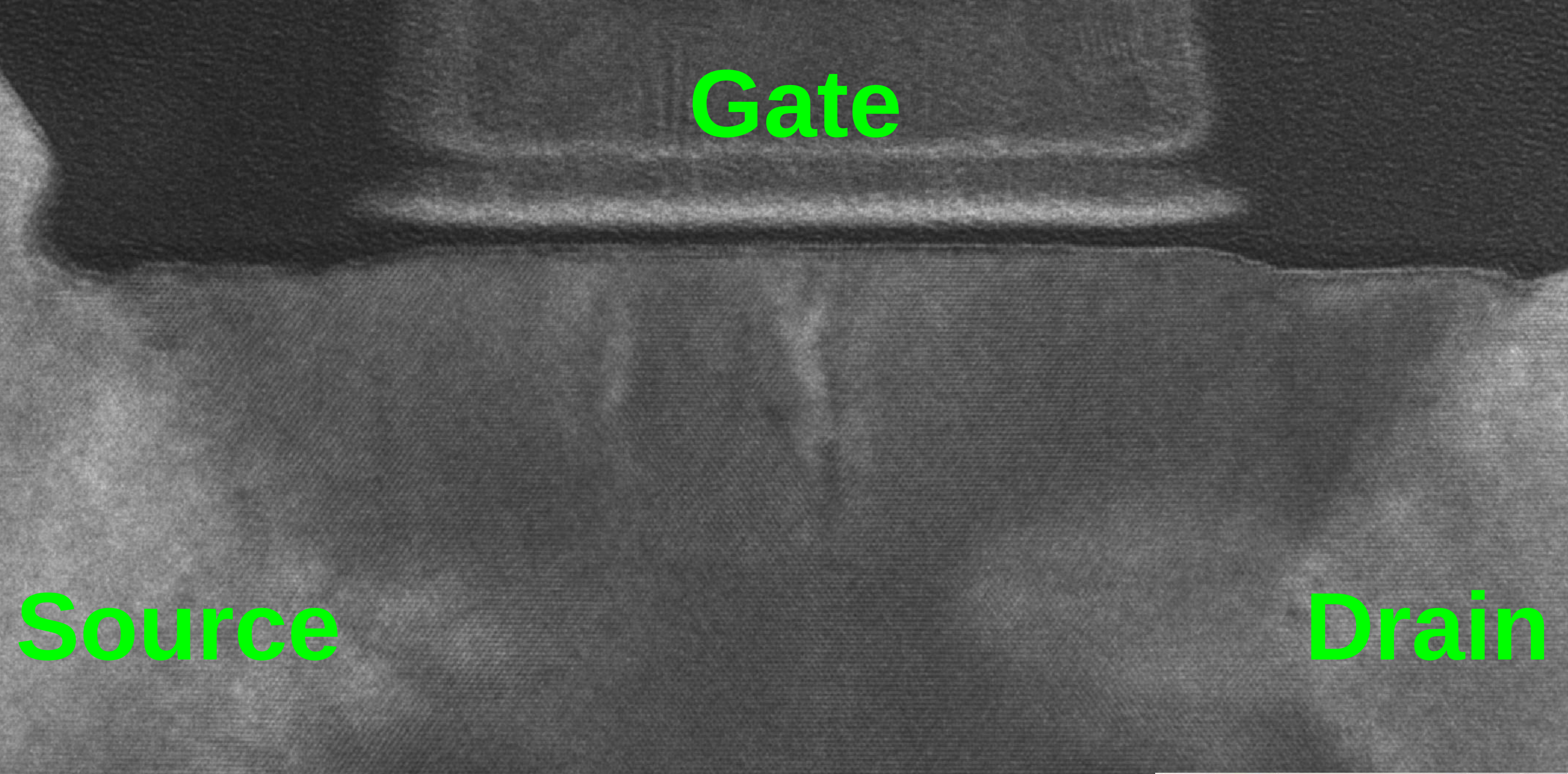

Microscope: JEOL ARM 1250

Quantitative DIH of 45nm CMOS transistor structure

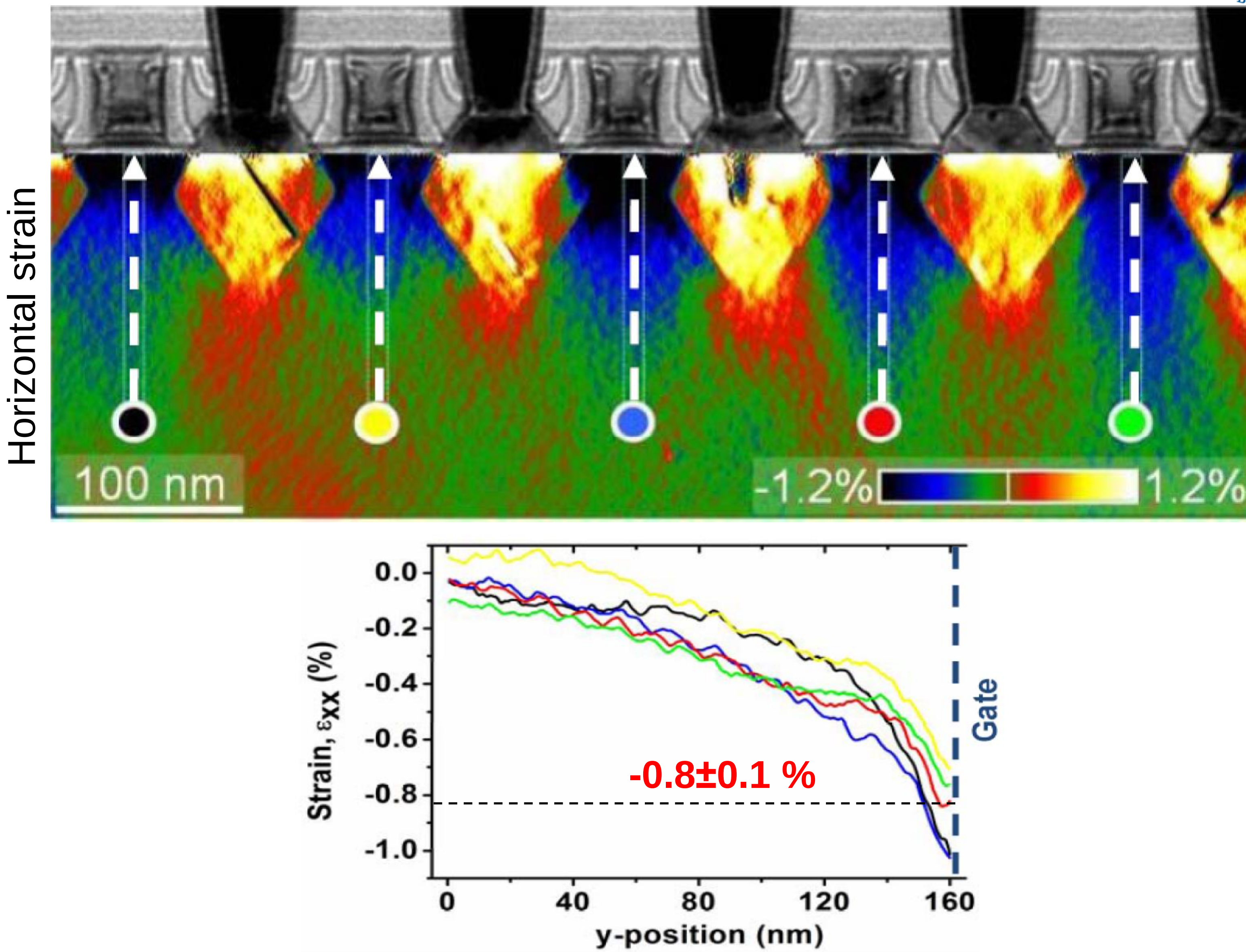

C. T. Koch et al, APL **96** (2010) 091901

Strain Mapping without Reference Area: InGaN QWs

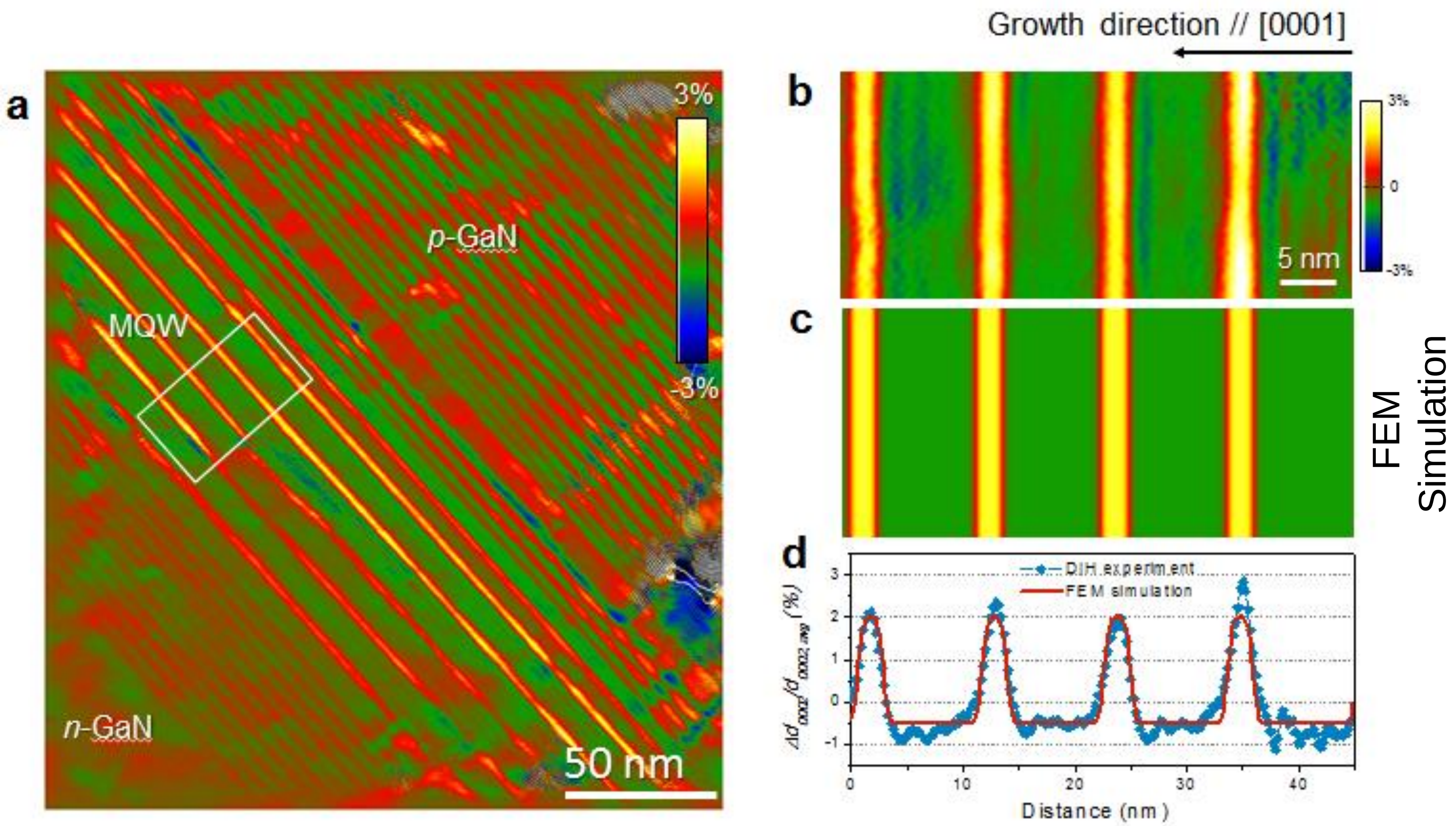

K. Song et al., in preparation

Summary

- Large-angle rocking curve information helps to
  - solve the crystallographic phase problem
  - allows automated acquisition of 3D diffraction information
  - reveals shape transform of nanocrystals
- Aberration compensation is very important when rocking to large angles
- Local variations in lattice constant can also be retrieved by (inline) holographic approaches